



# Complete systems of inequalities relating the perimeter, the area and the Cheeger constant of planar domains

Ilias Ftouhi

## ► To cite this version:

Ilias Ftouhi. Complete systems of inequalities relating the perimeter, the area and the Cheeger constant of planar domains. 2020. hal-03006019v2

**HAL Id: hal-03006019**

**<https://hal.science/hal-03006019v2>**

Preprint submitted on 23 Nov 2020 (v2), last revised 17 Jul 2022 (v6)

**HAL** is a multi-disciplinary open access archive for the deposit and dissemination of scientific research documents, whether they are published or not. The documents may come from teaching and research institutions in France or abroad, or from public or private research centers.

L'archive ouverte pluridisciplinaire **HAL**, est destinée au dépôt et à la diffusion de documents scientifiques de niveau recherche, publiés ou non, émanant des établissements d'enseignement et de recherche français ou étrangers, des laboratoires publics ou privés.

# Complete systems of inequalities relating the perimeter, the area and the Cheeger constant of planar domains

Ilias Ftouhi

November 23, 2020

## Abstract

We are interested in finding complete systems of inequalities between the perimeter  $P$ , the area  $|\cdot|$  and the Cheeger constant  $h$  of planar sets. To do so, we study the so called Blaschke-Santaló diagram of the triplet  $(P, |\cdot|, h)$  for different classes of domains: simply connected sets, convex sets and convex polygons with at most  $N$  sides. We are able to completely determine the diagram in the latter cases except for the class of convex  $N$ -gons when  $N \geq 5$  is odd: therein, we show that the external boundary of the diagram is given by the curves of two continuous and strictly increasing functions, we give an explicit formula of the lower one and provide a numerical method to obtain the upper one. We finally give some applications of the results and methods developed in the present paper.

**Keywords:** Cheeger constant, complete systems of inequalities, Blaschke-Santaló diagrams, convex sets, sharp spectral inequalities.

**AMS classification::** 52A10, 52A40, 49R99, 65K15

## Contents

<b>1</b>	<b>Introduction and main results</b>	<b>1</b>
<b>2</b>	<b>Classical results and preliminaries</b>	<b>6</b>
2.1	Classical results . . . . .	6
2.2	Preliminary lemmas . . . . .	6
<b>3</b>	<b>Proof of the main results</b>	<b>10</b>
3.1	Proof of inequality (5) . . . . .	10
3.2	Proof of the second assertion of Theorem 1.1 (convex sets) . . . . .	11
3.3	Proof of the first assertion of Theorem 1.1 (simply connected sets) . . . . .	13
3.4	Proof of inequality (7) . . . . .	14
3.5	Proof of Theorem 1.2 . . . . .	14
3.5.1	If $N = 3$ . . . . .	14
3.5.2	If $N$ is even . . . . .	15
3.5.3	If $N$ is odd . . . . .	17
<b>4</b>	<b>Numerical simulations</b>	<b>22</b>
4.1	Parameterization of the domains . . . . .	22
4.2	Computation of the gradients . . . . .	23
4.3	Results . . . . .	23
<b>5</b>	<b>Some applications</b>	<b>25</b>
5.1	First application . . . . .	25
5.2	Second application: on the stability of the Cheeger constant of polygons . . . . .	25

## 1 Introduction and main results

Let  $\Omega$  be a bounded subset of  $\mathbb{R}^n$  (where  $n \geq 2$ ). The Cheeger problem consists of studying the following minimization problem:

$$h(\Omega) := \inf \left\{ \frac{P(E)}{|E|} \mid E \text{ measurable and } E \subset \Omega \right\}, \quad (1)$$

where  $P(E)$  is the distributional perimeter of  $E$  measured with respect to  $\mathbb{R}^n$  (see for example [24] for definitions) and  $|E|$  is the  $n$ -dimensional Lebesgue measure of  $E$ . The quantity  $h(\Omega)$  is called *the Cheeger constant of  $\Omega$*  and any set  $C_\Omega \subset \Omega$  for which the infimum is attained is called a *Cheeger set of  $\Omega$* .

Since the early work of Jeff Cheeger [12], the study of the Cheeger problem has interested various authors, we refer to [24] for an introductory survey on the subject. We recall that every bounded domain  $\Omega$  with Lipschitz boundary admits at least one Cheeger set  $C_\Omega$ , see for example [24, Proposition 3.1]. In [1], the authors prove uniqueness of the Cheeger set when  $\Omega \subset \mathbb{R}^n$  is convex, but as far as we know there is no complete characterization of  $C_\Omega$  in the case of higher dimensions  $n \geq 3$  (even when convexity is assumed), in contrary with the planar case which was treated by Bernd Kawohl and Thomas Lachand-Robert in [20] where a complete description of the Cheeger sets of planar convex domains is given in addition to an algorithm to compute the Cheeger constant of convex polygons. We finally refer to [22, 21, 23] for recent results in larger classes of sets.

In this paper we are interested in describing all possible geometrical inequalities involving the perimeter, the volume and the Cheeger constant of a given planar shape. This is equivalent to study a so called Blaschke-Santaló diagram of the triplet  $(P, |\cdot|, h)$ .

A Blaschke-Santaló diagram is a tool that allows to visualize all possible inequalities between three quantities depending on the shape of a set: it was named as a reference to [26, 3], where the authors were looking for the description of inequalities involving three geometrical quantities for a given convex set. Afterward, this diagrams have been extensively studied especially for the class of planar convex sets. We refer to [18] for more details and various examples.

For more precision, let us define the Blaschke-Santaló diagrams we are interested in in this paper: given  $\mathcal{F}$  a class of measurable sets of  $\mathbb{R}^2$ , we define

$$\begin{aligned} \mathcal{D}_{\mathcal{F}} &:= \left\{ (x, y) \in \mathbb{R}^2, \exists \Omega \in \mathcal{F} \text{ such that } |\Omega| = 1, P(\Omega) = x, h(\Omega) = y \right\} \\ &:= \left\{ (P(\Omega), h(\Omega)), \Omega \in \mathcal{F}, |\Omega| = 1 \right\}. \end{aligned}$$

We note that thanks to the following homothety properties

$$\forall t > 0, \quad h(t\Omega) = \frac{h(\Omega)}{t}, \quad |t\Omega| = t^2|\Omega| \quad \text{and} \quad P(t\Omega) = tP(\Omega),$$

one can give a scaling invariant formulation of the diagram:

$$\begin{aligned} \mathcal{D}_{\mathcal{F}} &= \left\{ (x, y) \in \mathbb{R}^2, \exists \Omega \in \mathcal{F} \text{ such that } P(\Omega)/|\Omega|^{1/2} = x, |\Omega|^{1/2}h(\Omega) = y \right\} \\ &= \left\{ \left( \frac{P(\Omega)}{|\Omega|^{1/2}}, |\Omega|^{1/2}h(\Omega) \right), \Omega \in \mathcal{F} \right\} \end{aligned}$$

In the whole paper, we denote:

- $\mathcal{K}^2$  the set of planar non-empty convex sets,
- $\mathcal{P}_N$  the set of convex polygons of at most  $N$  sides,
- $B$  the disk of unit area,
- $R_N$  a regular polygon of  $N$  sides and unit area,
- $d^H$  the Hausdorff distance, see for example [16, Chapter 2] for definition and more details.
- $d(\Omega)$  and  $r(\Omega)$  respectively the diameter and inradius of the set  $\Omega \subset \mathbb{R}^2$ .

We are aiming at describing all possible inequalities relating  $P$ ,  $|\cdot|$  and  $h$  in different classes of planar sets and then describing the associated Blaschke-Santaló diagrams. Let us first state the inequalities we already know; if  $\Omega$  is measurable, we have :

- the isoperimetric inequality:

$$\frac{P(\Omega)}{|\Omega|^{1/2}} \geq \frac{P(B)}{|B|^{1/2}} = 2\sqrt{\pi}, \quad (2)$$

- a consequence of the definition of the Cheeger constant

$$h(\Omega) = \inf_{E \subset \Omega} \frac{P(E)}{|E|} \leq \frac{P(\Omega)}{|\Omega|}, \quad (3)$$

- a Faber-Krahn type inequality:

$$|\Omega|^{1/2}h(\Omega) \geq |B|^{1/2}h(B) = \frac{P(B)}{|B|^{1/2}} = 2\sqrt{\pi}, \quad (4)$$

this inequality readily follows from definition (1) and the isoperimetric inequality. Indeed:

$$|\Omega|^{1/2}h(\Omega) = h(\Omega') = \frac{P(C_{\Omega'})}{|C_{\Omega'}|} \geq \frac{P(C_{\Omega'}^*)}{|C_{\Omega'}^*|} \geq h(B) = P(B) = 2\sqrt{\pi},$$

where  $\Omega' := |\Omega|^{-1/2}\Omega$  and  $C_{\Omega'}^*$  is a ball with the same volume as  $C_{\Omega'}$ .

Note that each inequality may be visualised in the Blaschke-Santaló diagram as the curve of a given function, see Figure 2, and that the first inequality may be obtained by combining the second and third ones.

It is natural to wonder if there are other inequalities, we prove that this is not the case for general sets, indeed, in Theorem 1.1 we give the explicit description of the Blaschke-Santaló diagram in the case of simply connected domains (see also Figure 2). One could wonder why we chose to work with the class of simply connected domains: the main reason is that for any subclass of measurable domains that contains the simply connected ones, the diagram is the same.

Now, let us provide complete descriptions of the Blaschke-Santaló diagram of the triplet  $(P, h, |\cdot|)$  for both the classes  $\mathcal{S}^2$  of planar simply connected sets and  $\mathcal{K}^2$  of planar convex sets.

**Theorem 1.1.** Denote  $x_0 = P(B) = 2\sqrt{\pi}$ .

1. The diagram of the class  $\mathcal{S}$  of planar simply connected domains is given by:

$$\mathcal{D}_{\mathcal{S}^2} = \{(x_0, x_0)\} \cup \{(x, y) \mid x \geq x_0 \text{ and } x_0 < y \leq x\}.$$

2. The diagram of the class  $\mathcal{K}$  of planar convex domains is given by:

$$\mathcal{D}_{\mathcal{K}^2} = \left\{ (x, y) \mid x \geq x_0 \text{ and } \frac{x}{2} + \sqrt{\pi} \leq y \leq x \right\}.$$

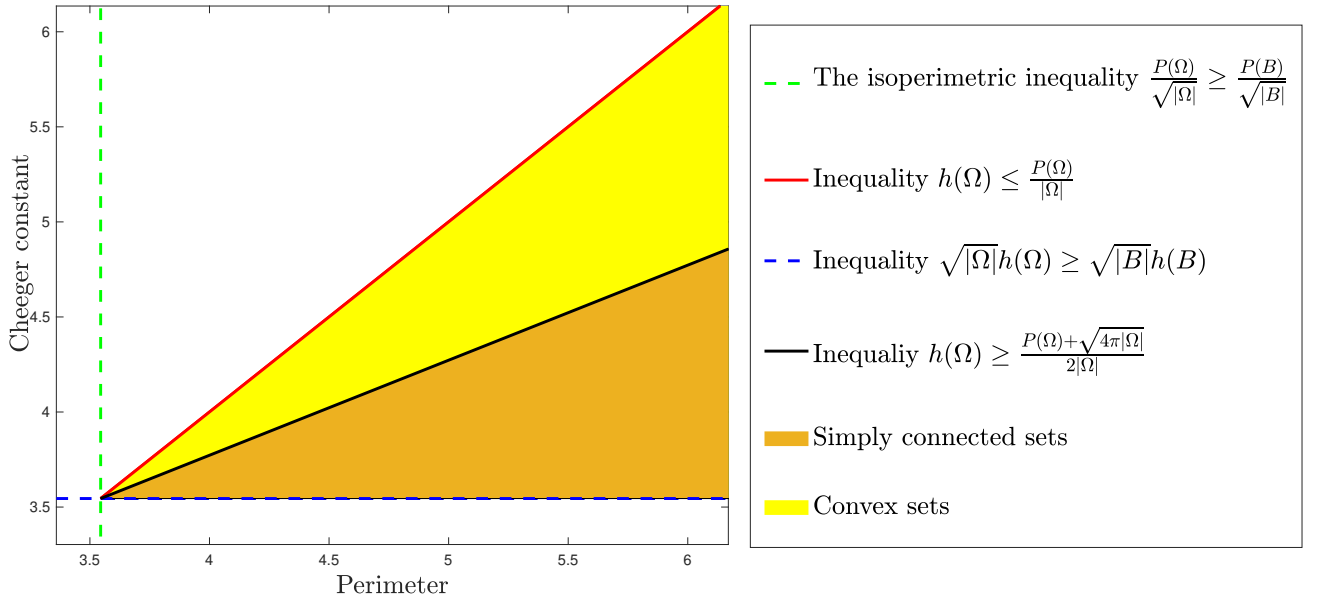


Figure 1: Blaschke-Santaló diagrams for the classes of simply connected sets and convex sets.

We note that by taking advantage of inequalities (2) and (4), it is also classical to represent Blaschke-Santaló diagram as subset of  $[0, 1]^2$ , in our situation, this means to consider sets:

$$\mathcal{D}'_{\mathcal{F}} := \left\{ (X, Y) \mid \exists \Omega \in \mathcal{F} \text{ such as } |\Omega| = 1 \text{ and } (X, Y) = \left( \frac{P(B)}{P(\Omega)}, \frac{h(B)}{h(\Omega)} \right) \right\} \subset [0, 1]^2,$$

where  $\mathcal{F}$  is a given class of planar sets. With this parametrization, Blaschke-Santaló diagrams for the classes  $\mathcal{S}$  and  $\mathcal{K}^2$  are given by the following sets:

$$\begin{cases} \mathcal{D}'_{\mathcal{S}^2} &= \{(1, 1)\} \cup \{(X, Y) \mid X \in (0, 1) \text{ and } X \leq Y < 1\}, \\ \mathcal{D}'_{\mathcal{K}^2} &= \{(X, Y) \mid X \in (0, 1] \text{ and } X \leq Y \leq \frac{2X}{1+X}\}, \end{cases}$$

which are represented in Figure 2.

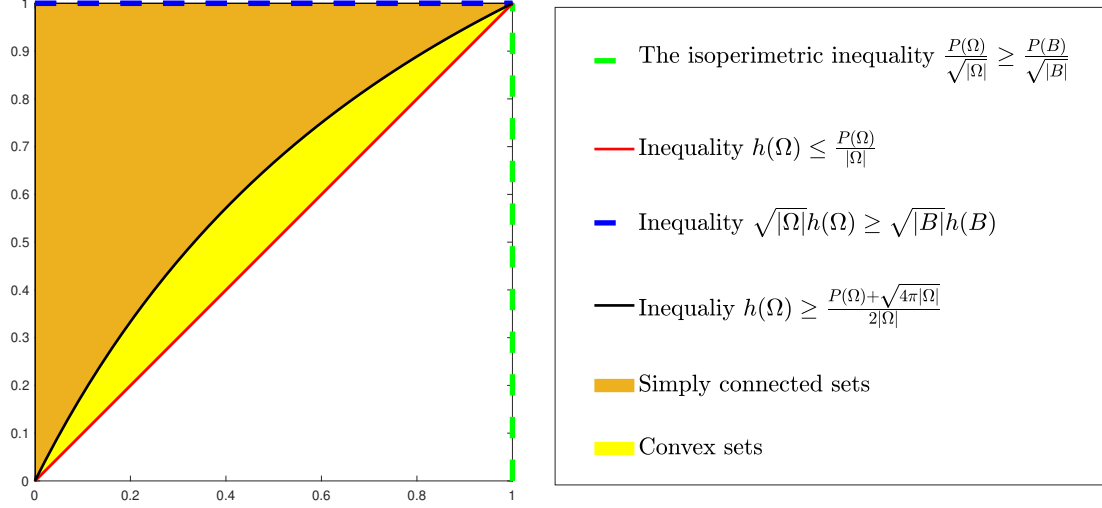


Figure 2: Blaschke-Santaló diagrams for the classes of simply connected sets and convex sets represented in  $[0, 1]^2$ .

Let us give some comments on the latter results:

- One major step in the study of the diagram of convex sets is to prove the following sharp inequality:

$$\forall \Omega \in \mathcal{K}^2, \quad h(\Omega) \geq \frac{P(\Omega) + \sqrt{4\pi|\Omega|}}{2|\Omega|}, \quad (5)$$

where equality occurs for example for circumscribed polygons (ie. those whose sides touch their incircles) and more generally for sets which are homothetical to their form bodies<sup>1</sup>.

- Inequality (5) is rather easy to prove when the convex  $\Omega$  is a Cheeger-regular polygon (that is, its Cheeger set touches all of its sides), see [9, Remark 32], but much difficult to prove for general convex sets as shown in the present paper. We also note that this inequality may be seen as a quantitative isoperimetric inequality for the Cheeger constant of convex planar sets: indeed, it could be written in the following form

$$\forall \Omega \in \mathcal{K}^2, \quad |\Omega|^{1/2}h(\Omega) - |B|^{1/2}h(B) \geq \frac{1}{2} \left( \frac{P(\Omega)}{|\Omega|^{1/2}} - \frac{P(B)}{|B|^{1/2}} \right) \geq 0.$$

We refer to [15, 19] for some examples of quantitative inequalities for the Cheeger constant.

At last, we note in Section 5.1 that inequality (5) is stronger than a classical result [8, Theorem 3] due to R. Brooks and P. Waksman. It also improves in the planar case a more recent estimate given in [6, Corollary 5.2], that states that for any open bounded convex set  $\Omega \subset \mathbb{R}^n$ , where  $n \geq 2$ , one has:

$$h(\Omega) \geq \frac{1}{n} \times \frac{P(\Omega)}{|\Omega|}.$$

- We note that the first statement of Theorem 1.1 asserts that (3) and (4) form a complete system of inequalities of the triplet  $(P, h, |\cdot|)$  in any class of sets that contains the class  $\mathcal{S}$ . Meanwhile, the second one asserts that this is no longer the case for the class  $\mathcal{K}^2$  of planar convex sets, where estimates (3) and (5) are then shown to be forming a complete system of inequalities of the triplet  $(P, h, |\cdot|)$ .

<sup>1</sup>We refer to [27, Page 386] for the definition of form bodies.

- We finally note that due to technical convenience, we first show the second assertion (diagram of convex sets) and then use it to prove the first one (diagram of simply connected sets).

Now, let us focus on the class of convex polygons. We give an improvement of inequality (3) in the class  $\mathcal{P}_N$  of convex polygons of at most  $N$  sides, where  $N \geq 3$ . We recall that since triangles are inscribed polygons, one has:

$$\forall \Omega \in \mathcal{P}_3, \quad h(\Omega) = \frac{P(\Omega) + \sqrt{4\pi|\Omega|}}{2|\Omega|}. \quad (6)$$

As for the case  $N \geq 4$ , we prove the following sharp upper bound for the Cheeger constant of convex  $N$ -gons.

Take  $N \geq 4$ , we have

$$\forall \Omega \in \mathcal{P}_N, \quad h(\Omega) \leq \frac{P(\Omega) + \sqrt{P(\Omega)^2 + 4(\pi - N \tan \frac{\pi}{N})|\Omega|}}{2|\Omega|}, \quad (7)$$

with equality if and only if  $\Omega$  is Cheeger-regular and all of its angles are equal (to  $(N-2)\pi/N$ ). Equality is also attained asymptotically by the following family  $((0, 1) \times (0, d))_{d \geq 1}$  of rectangles when  $d \rightarrow +\infty$ .

It is interesting to note that inequalities (5) and (7) form a complete system of inequalities of the triplet  $(P, |\cdot|, h)$  in the class  $\mathcal{P}_N$  if and only if  $N$  is even. In the following Theorem 1.2, we give an explicit description of the diagram of convex polygons when  $N$  is even or equal to 3, give the explicit description of the lower boundary and provide some qualitative results on the upper one when  $N$  is odd. In Section 4, we perform some numerical simulations in order to numerically find the extremal upper domains and thus give a numerical description of the upper boundary.

**Theorem 1.2.** *Take  $N \geq 3$ , we recall that  $R_N$  denotes a regular polygon of  $N$  sides and unit area.*

*We denote*

$$\mathcal{D}_N := \left\{ \left( \frac{P(\Omega)}{|\Omega|^{1/2}}, |\Omega|^{1/2} h(\Omega) \right) \mid \Omega \in \mathcal{P}_N \right\}.$$

*We distinguish the following cases:*

- if  $N = 3$ , we have

$$\mathcal{D}_3 = \left\{ \left( x, \frac{x}{2} + \sqrt{\pi} \right) \mid x \geq P(R_3) \right\}$$

- if  $N$  is even, then

$$\mathcal{D}_N = \left\{ (x, y) \mid x \geq P(R_N) \text{ and } \frac{x}{2} + \sqrt{\pi} \leq y \leq f_N(x) \right\},$$

$$\text{where } f_N : x \in [P(R_N), +\infty) \mapsto \frac{x + \sqrt{x^2 + 4(\pi - N \tan \frac{\pi}{N})}}{2}.$$

- if  $N \geq 5$  is odd, we provide a qualitative description of the boundary of the diagram  $\mathcal{D}_N$ :

- The lower boundary is given by the half line:

$$\{(x, y) \mid x \geq P(R_N) \text{ and } y = x/2 + \sqrt{\pi}\},$$

*which is included in the diagram  $\mathcal{D}_N$ .*

- The upper boundary is given by the curve:

$$\{(x, y) \mid x \geq P(R_N) \text{ and } y = g_N(x)\},$$

*which is also included in the diagram  $\mathcal{D}_N$ , where  $g_N$  is a continuous and strictly increasing function such that  $g_N \leq f_N$  on  $[P(R_N), +\infty)$ . Moreover, there exists  $c_N \geq b_N > P(R_N)$  such that  $g_N = f_N$  on  $[P(R_N), b_N]$  and  $g_N < f_N$  on  $[c_N, +\infty)$ .*

The paper is organized as follows: Section 2 contains two subsections, in the first one we recall some classical results needed for the proofs, in the second one we state and prove some preliminary lemmas which are also interesting for themselves. The proofs of the main results are given in Section 3. Then, we provide some numerical results on the diagrams  $\mathcal{D}_N$  in Section 4. Finally, we give some applications of the results and ideas of the present paper in Section 5.

## 2 Classical results and preliminaries

### 2.1 Classical results

In this subsection, we recall some classical results that are used throughout the whole paper.

**Theorem 2.1.** [14, Th.2 and Remark 3]

Take  $N \geq 3$  and  $\Omega \subset \mathbb{R}^2$  a convex polygon of  $N$  sides. We define:

$$T(\Omega) := \sum_{i=1}^N \frac{1}{\tan \frac{\alpha_i}{2}},$$

where  $\alpha_i \in (0, \pi]$  are the inner angles of  $\Omega$ . We have the following estimates:

$$N \tan \frac{\pi}{N} \leq T(\Omega) \leq \frac{P(\Omega)^2}{4|\Omega|}. \quad (8)$$

The lower bound is attained if and only if all the angles  $\alpha_i$  are equal (to  $\frac{N-2}{2N}\pi$ ), meanwhile the upper one is an equality if and only if the polygon  $\Omega$  is circumscribed.

**Remark 2.2.** The lower bound is a simple application of Jensen's inequality to the function  $\cotan$  which is strictly convex on  $(0, \pi/2)$ . On the other hand, since  $N \tan \frac{\pi}{N} > \pi$ , the upper estimate may be seen as an improvement of the isoperimetric inequality for convex polygons. We refer to [14] for a detailed proof of Theorem 2.1.

Let us now recall some classical and important results on the Cheeger problem for planar convex sets.

**Theorem 2.3.** [20, Th. 1] There exists a unique value  $t = t^* > 0$  such that  $|\Omega_{-t}| = \pi t^2$ . Then  $h(\Omega) = 1/t^*$  and the Cheeger set of  $\Omega$  is  $C_\Omega = \Omega_{-t^*} + t^* B_1$ , with  $B_1$  denoting the unit disk.

**Theorem 2.4.** [20, Th. 3] If  $\Omega$  is a Cheeger-regular polygon (that is, its Cheeger set touches every side of  $\Omega$ ), then:

$$h(\Omega) = \frac{P(\Omega) + \sqrt{P(\Omega)^2 - 4(T(\Omega) - \pi)|\Omega|}}{2|\Omega|}.$$

It is natural to wonder if equality holds also for some Cheeger irregular polygons: in Lemma 2.5, we prove that there is only an inequality and that the equality case occurs only when the polygon is Cheeger regular.

### 2.2 Preliminary lemmas

In this section we prove some important Lemmas that we use in Section 3 for the proofs of the main results.

The following Lemma shows that the equality of Theorem 2.3 which is valid for Cheeger regular polygons becomes an inequality for general polygons and thus gives an upper bound of the Cheeger constant of polygons that we use to prove inequality (7).

**Lemma 2.5.** If  $\Omega$  is a polygon, one has:

$$h(\Omega) \leq \frac{P(\Omega) + \sqrt{P(\Omega)^2 - 4(T(\Omega) - \pi)|\Omega|}}{2|\Omega|},$$

with equality if and only if  $\Omega$  is Cheeger-regular.

*Proof.* Let us denote:

$$F(\Omega) := \frac{P(\Omega) + \sqrt{P(\Omega)^2 - 4(T(\Omega) - \pi)|\Omega|}}{2|\Omega|}.$$

The key of the proof is to understand the graphical interpretation of  $h(\Omega)$  and  $F(\Omega)$ . Indeed:

- $1/h(\Omega)$  is the (unique) solution of the equation  $g(t) := |\Omega_{-t}| - \pi t^2$  in  $[0, r(\Omega)]$ ,
- $1/F(\Omega)$  is the smallest solution of the equation  $f(t) := |\Omega| - P(\Omega)t + T(\Omega)t^2 - \pi t^2$  in  $[0, r(\Omega)]$ ,

where  $r(\Omega)$  is the inradius of  $\Omega$ .

The number of sides of the inner sets  $\Omega_t$  of a polygon is decreasing with respect to  $t \geq 0$ . Actually, the function  $t \in [0, r(\Omega)] \mapsto n(t)$  (where  $n(t)$  is the number of sides of  $\Omega_{-t}$ ) is a piece-wise constant decreasing function. We introduce the sequence  $0 = t_0 < t_1 < \dots < t_N = r(\Omega)$ , where  $N \in \mathbb{N}^*$ , such that:

$$\forall k \in \llbracket 0, N-1 \rrbracket, \forall t \in [t_k, t_{k+1}) \quad n(t) = n(0) - k.$$

Let us take  $t \in [0, r(\Omega)]$  and a  $k \in \llbracket 1, N \rrbracket$ . We have:

$$\begin{aligned} |\Omega_{t_k}| - (t - t_k)P(\Omega_{-t_k}) + (t - t_k)^2 T(\Omega_{-t_k}) &= |\Omega_{-t_{k-1}}| - (t_k - t_{k-1})P(\Omega_{-t_{k-1}}) + (t_k - t_{k-1})^2 T(\Omega_{-t_{k-1}}) \\ &\quad - (t - t_k)(P(\Omega_{-t_{k-1}}) - 2(t_k - t_{k-1})T(\Omega_{-t_{k-1}})) + (t - t_k)^2 T(\Omega_{-t_k}) \\ &> |\Omega_{-t_{k-1}}| - (t - t_{k-1})P(\Omega_{-t_{k-1}}) + (t - t_{k-1})^2 T(\Omega_{-t_{k-1}}), \end{aligned}$$

where we used Steiner formulas for inner convex polygons for the first equality and the fact that  $T(\Omega_{-t_{k-1}}) < T(\Omega_{-t_k})$  for the inequality (see [20, Section 5.]). By straightforward induction we show that for every  $k \in \llbracket 1, N \rrbracket$ , one has:

$$\forall t \in [0, r(\Omega)], \quad |\Omega_{t_k}| - (t - t_k)P(\Omega_{-t_k}) + (t - t_k)^2 T(\Omega_{-t_k}) \geq |\Omega| - tP(\Omega) + t^2 T(\Omega). \quad (9)$$

Now, let us take  $k \in \llbracket 0, N \rrbracket$  and  $t \in [t_k, t_{k+1})$ . We have:

$$\begin{aligned} g(t) &:= |\Omega_{-t}| - \pi t^2 = |(\Omega_{-t_k})_{-(t-t_k)}| - \pi t^2 = |\Omega_{t_k}| - (t - t_k)P(\Omega_{-t_k}) + (t - t_k)^2 T(\Omega_{-t_k}) - \pi t^2 \\ &\geq |\Omega| - tP(\Omega) + t^2 T(\Omega) - \pi t^2 =: f(t), \end{aligned}$$

where equality  $g(t) = f(t)$  holds only on  $[0, t_1]$ .

Finally

$$\begin{cases} \forall t \in [0, t_1], & g(t) = f(t), \\ \forall t \in (t_1, r(\Omega)), & g(t) > f(t) \end{cases}$$

where equality holds only on  $[0, t_1]$ . This tells us that  $1/h(\Omega)$ , the first zero of  $g$  on  $[0, r(\Omega)]$ , is actually larger than  $1/F(\Omega)$ , the first zero of  $f$ , with equality if and only if the first zero of  $g$  is in  $[0, t_1]$ , which is the case if and only when the polygon  $\Omega$  is Cheeger-regular (see [20, Theorem 3.]). This ends the proof.  $\square$

Since inequality (5) is quite easy to obtain for Cheeger regular polygons (because in this case we have an explicit formula for the Cheeger constant in terms of the perimeter, the area and the inner angles), it is natural when dealing with general polygons to try to come back the latter case of Cheeger regular ones. The following Lemma shows how to deform a given polygon to a Cheeger regular while preserving its Cheeger constant, increasing its perimeter and decreasing its area, this allows as shown in **Step 2** of Section 3.1 to prove inequality (5) for the case of general polygons.

**Lemma 2.6.** *Let  $\Omega$  be a polygon. There exists a Cheeger-regular polygon  $\tilde{\Omega}$  such that:  $|\Omega| \geq |\tilde{\Omega}|$ ,  $P(\Omega) \leq P(\tilde{\Omega})$  and  $h(\Omega) = h(\tilde{\Omega})$ .*

*Proof.* If  $\Omega$  is Cheeger regular we take  $\tilde{\Omega} = \Omega$ . Let  $\Omega$  be a Cheeger irregular polygon. We give an algorithm of deforming  $\Omega$  into a Cheeger regular polygon with the same Cheeger set (thus also the same Cheeger value), larger perimeter and smaller area.

Since  $\Omega$  is Cheeger irregular, there exists three consecutive vertices that we denote  $X$ ,  $Y$  and  $Z$  such that at least one (may be both) of the sides  $XY$  and  $YZ$  does not touch the Cheeger set  $C_\Omega$ .

#### **First step: using parallel chord movements**

We begin by the case where both the sides  $XY$  and  $YZ$  does not touch  $C_\Omega$ . We use a parallel chord movement. More precisely, we move  $Y$  along the line passing through  $Y$  and being parallel to the line  $(XZ)$ . This way, the volume is preserved, and the perimeter must increase when moving  $Y$  away from the perpendicular bisector of  $[XZ]$  (which is possible at least in one direction). We assume without loss of generality that the direction which increases the perimeter is from  $Z$  to  $X$  (see Figure 3). We then move  $Y$  until one the following cases occurs:

1.  $(XY)$  becomes colinear to the other side of extremity  $X$ .
2.  $[YZ]$  touches the boundary of  $C_\Omega$ .



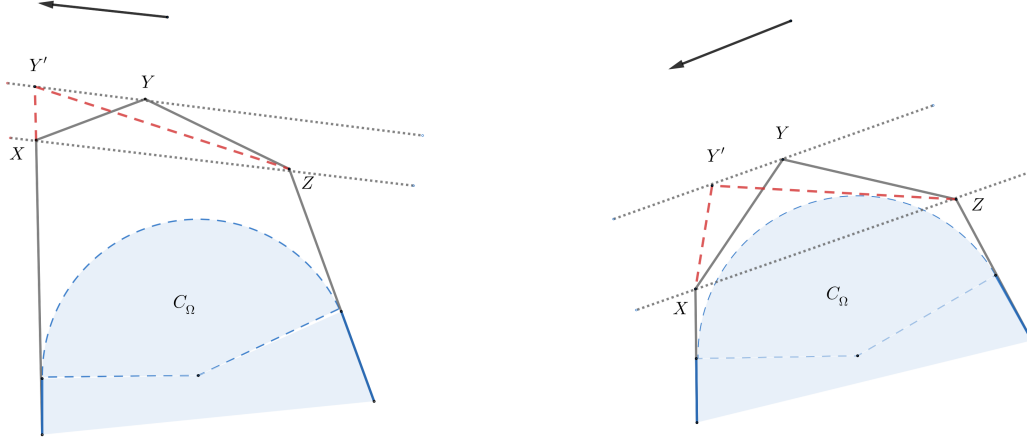


Figure 3: Case 1 on the left and case 2 on the right.

In both cases, the number of sides that do not touch  $\partial C_\Omega$  is diminished by one, while the area and the Cheeger constant are conserved and the perimeter is increased.

We iterate the latter process for all vertices which are extremities of two sides that do not touch  $\partial C_\Omega$ , since the number of vertices is finite, in a finite number of steps we obtain a polygon where there are no consecutive sides that do not touch  $\partial C_\Omega$ .

#### **Second step: rotating the remaining sides**

The second step is to "rotate" the remaining sides that do not touch  $\partial C_\Omega$  in such a way to make them touch it (see Figure 4), in order to get a Cheeger-regular polygon with the same Cheeger constant, larger perimeter and smaller area. This kind of deformations was inspired from the work of D. Bucur and I. Fragala [9].

We denote by  $\alpha_1, \alpha_2 \in (0, \pi)$  the inner angles of the polygon  $\Omega$  respectively associated to the vertices  $X$  and  $Y$ ,  $O$  the mid-point of the side  $[XY]$ ,  $t$  the angle of our "rotation" and  $X_t$  and  $Y_t$  the vertices of the obtained polygon  $\Omega_t$  (see Figure 4).

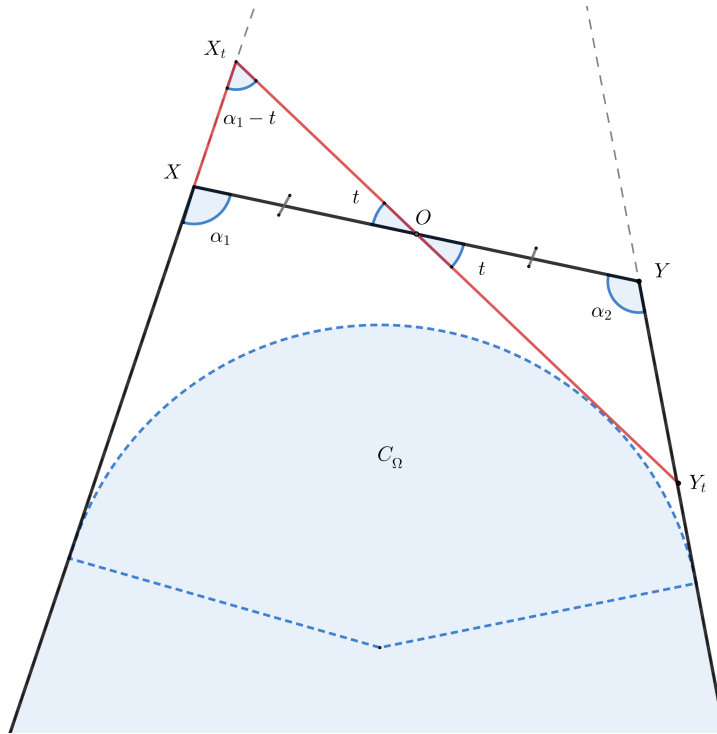


Figure 4: Rotation of the free side along its midpoint.

Without loss of generality, we assume that  $\alpha_2 \geq \alpha_1$  and  $t \geq 0$ . It is classical that  $\Omega$  and  $\Omega_t$  have the same Cheeger constant, moreover if the side  $[XY]$  is not touching  $\partial C_\Omega$  then  $\alpha_1 + \alpha_2 \geq \pi$  (see [20, Section 5]).

By using the sinus formula on triangles  $OXX_t$  and  $OYY_t$ , we have:

$$\begin{cases} AX_t = a \frac{\sin t}{\sin(\alpha_1 - t)} & \text{and} & OX_t = a \frac{\sin \alpha_1}{\sin(\alpha_1 - t)} \\ BY_t = a \frac{\sin t}{\sin(\alpha_2 + t)} & \text{and} & OY_t = a \frac{\sin \alpha_2}{\sin(\alpha_2 + t)} \end{cases}$$

where  $a := OX = XY/2$ .

Moreover, if we denote by  $S_{OXX_t}$  and  $S_{OYY_t}$  the areas of the triangles  $OXX_t$  and  $OYY_t$ , we have:

$$\begin{aligned} |\Omega_t| - |\Omega| &= S_{OXX_t} - S_{OYY_t} \\ &= \frac{1}{2} OX \times OX_t \sin t - \frac{1}{2} OY \times OY_t \sin t \\ &= \frac{a^2}{2} \left( \frac{\sin \alpha_1}{\sin(\alpha_1 - t)} - \frac{\sin \alpha_2}{\sin(\alpha_2 + t)} \right) \sin t \\ &= \frac{a^2 \sin^2 t \sin(\alpha_1 + \alpha_2)}{2 \sin(\alpha_1 - t) \sin(\alpha_2 + t)} \leq 0 \end{aligned}$$

because  $t \geq 0$ ,  $\alpha_1 - t, \alpha_2 + t \in [0, \pi]$  and  $\alpha_1 + \alpha_2 \in [\pi, 2\pi]$ , because  $\Omega$  is a convex polygon and the side  $[XY]$  does not touch  $\partial C_\Omega$  (see [20, Section 5]).

For the perimeters, we have:

$$\begin{aligned} P(\Omega_t) - P(\Omega) &= XX_t + OX_t + OY_t - XY - YY_t \\ &= a \left( \frac{\sin t}{\sin(\alpha_1 - t)} + \frac{\sin \alpha_1}{\sin(\alpha_1 - t)} + \frac{\sin \alpha_2}{\sin(\alpha_2 + t)} - 2 - \frac{\sin t}{\sin(\alpha_2 + t)} \right) \\ &= a \left( \frac{\sin t + \sin \alpha_1}{\sin(\alpha_1 - t)} + \frac{\sin \alpha_2 - \sin t}{\sin(\alpha_2 + t)} - 2 \right) \\ &= a \left( \frac{2 \sin \left( \frac{\alpha_1 + t}{2} \right) \cos \left( \frac{\alpha_1 - t}{2} \right)}{2 \sin \left( \frac{\alpha_1 - t}{2} \right) \cos \left( \frac{\alpha_1 - t}{2} \right)} + \frac{2 \sin \left( \frac{\alpha_2 - t}{2} \right) \cos \left( \frac{\alpha_2 + t}{2} \right)}{2 \sin \left( \frac{\alpha_2 + t}{2} \right) \cos \left( \frac{\alpha_2 + t}{2} \right)} - 2 \right) \\ &= a \left( \sqrt{\frac{\sin \left( \frac{\alpha_1 + t}{2} \right)}{\sin \left( \frac{\alpha_1 - t}{2} \right)}} - \sqrt{\frac{\sin \left( \frac{\alpha_1 - t}{2} \right)}{\sin \left( \frac{\alpha_1 + t}{2} \right)}} \right)^2 \geq 0. \end{aligned}$$

Finally, in a finite number of steps, we get a Cheeger-regular polygon  $\tilde{\Omega}$  such that:  $|\Omega| \geq |\tilde{\Omega}|$ ,  $P(\Omega) \leq P(\tilde{\Omega})$  and  $h(\Omega) = h(\tilde{\Omega})$ . □

Let us now recall the definition of a radial function: let  $\Omega$  be a starlike planar domain that contains the origin  $O$ . We define the radial function  $f_\Omega : \mathbb{R} \rightarrow \mathbb{R}$  of  $\Omega$  as follows:

$$\forall \theta \in \mathbb{R}, \quad f_\Omega(\theta) = \sup \left\{ t > 0 \mid t \begin{pmatrix} \cos \theta \\ \sin \theta \end{pmatrix} \in \Omega \right\}.$$

In the following Lemma we give some quantitative estimates for the Cheeger constant and area via radial functions, that will be used in the fourth step of Section 3.2.

**Lemma 2.7.** *Take  $\Omega_1$  and  $\Omega_2$  two starlike planar domains with radial functions  $f_1$  and  $f_2$  such that  $f_1, f_2 \geq r_0$ , where  $r_0 > 0$ .*

*We have:*

1.  $|h(\Omega_1) - h(\Omega_2)| \leq \frac{2}{r_0^2} \times \|f_1 - f_2\|_\infty$ .
2.  $||\Omega_1| - |\Omega_2|| \leq \pi \times \max(\|f_1\|_\infty, \|f_2\|_\infty) \times \|f_1 - f_2\|_\infty$

*Proof.* 1. The proof of this assertion inspired from [13, Proposition 1].

We denote  $d = \|f_1 - f_2\|_\infty$ , we have  $(1 + d/r_0)f_1 \geq (f_2 - d) + d = f_2$ , thus:

$$h(\Omega_1) \leq h \left( \frac{1}{1 + d/r_0} \Omega_2 \right) = \left( 1 + \frac{d}{r_0} \right) h(\Omega_2) \leq h(\Omega_2) + \frac{d}{r_0} h(B_{r_0}) = h(\Omega_2) + \frac{2d}{r_0^2},$$

where  $B_{r_0}$  is the disk of radius  $r_0$ .

By similar arguments we obtain:

$$h(\Omega_2) \leq h(\Omega_1) + \frac{2d}{r_0^2},$$

which proves the announced inequality.

2. We have

$$\begin{aligned} ||\Omega_1| - |\Omega_2|| &= \frac{1}{2} \times \left| \int_0^{2\pi} (f_1^2(\theta) - f_2^2(\theta)) d\theta \right| \\ &\leq \frac{1}{2} \int_0^{2\pi} (|f_1(\theta)| + |f_2(\theta)|) \times |f_1(\theta) - f_2(\theta)| d\theta \\ &\leq \pi \times \max(\|f_1\|_\infty, \|f_2\|_\infty) \times \|f_1 - f_2\|_\infty \end{aligned}$$

□

### 3 Proof of the main results

#### 3.1 Proof of inequality (5)

The proof is done in four steps:

##### Step 1: Cheeger-regular polygons

Even-though the inequality was already known in this case, we briefly recall the proof for sake of completeness.

Since  $\Omega$  is a Cheeger-regular polygon, by Theorem 2.4, we dispose of an explicit formula of its Cheeger constant, we then just have to use Theorem 2.1 to conclude.

We write:

$$h(\Omega) = \frac{P(\Omega) + \sqrt{P(\Omega)^2 - 4(T(\Omega) - \pi)|\Omega|}}{2|\Omega|} \geq \frac{P(\Omega) + \sqrt{P(\Omega)^2 - 4\left(\frac{P(\Omega)^2}{4|\Omega|} - \pi\right)|\Omega|}}{2|\Omega|} = \frac{P(\Omega) + \sqrt{4\pi|\Omega|}}{2|\Omega|}.$$

##### Step 2: General polygons

By Lemma 2.6, there exists  $\tilde{\Omega}$  a Cheeger-regular polygon such that:  $|\Omega| \leq |\tilde{\Omega}|$ ,  $P(\Omega) = P(\tilde{\Omega})$  and  $h(\Omega) = h(\tilde{\Omega})$ . Then, we get:

$$h(\Omega) = h(\tilde{\Omega}) \geq \frac{P(\tilde{\Omega}) + \sqrt{4\pi|\tilde{\Omega}|}}{2|\tilde{\Omega}|} = \frac{P(\tilde{\Omega})}{2|\tilde{\Omega}|} + \frac{\pi}{\sqrt{|\tilde{\Omega}|}} \geq \frac{P(\Omega)}{2|\Omega|} + \frac{\pi}{\sqrt{|\Omega|}} = \frac{P(\Omega) + \sqrt{4\pi|\Omega|}}{2|\Omega|}.$$

##### Step 3: General convex sets

By density of the polygons in  $\mathcal{K}^2$  and the continuity of the area, perimeter and Cheeger constant for the Hausdorff distance, we show that the inequality holds for general convex sets.

##### Step 4: Equality for sets that are homothetical to their form bodies

If  $\Omega$  is homothetical to its form body (which is in the case of circumscribed polygons), we have by using [27, (7.168)] and equality  $\frac{1}{2}r(\Omega)P(\Omega) = |\Omega|$ :

$$\forall t \in [0, r(\Omega)], \quad |\Omega_{-t}| = \left(1 - \frac{t}{r(\Omega)}\right)^2 |\Omega| = |\Omega| - P(\Omega)t + \frac{P(\Omega)^2}{4|\Omega|}.$$

Thus, by using Theorem 2.3 we obtain the equality:

$$h(\Omega) = \frac{P(\Omega) + \sqrt{4\pi|\Omega|}}{2|\Omega|}. \quad (10)$$

### 3.2 Proof of the second assertion of Theorem 1.1 (convex sets)

As explained in the introduction, inequalities (3) and (5) imply that

$$\mathcal{D}_{\mathcal{K}^2} \subset \left\{ (x, y) \mid x \geq x_0 \text{ and } \frac{1}{2}x + \sqrt{\pi} \leq y \leq x \right\}.$$

It remains to prove the reverse inclusion. The proof follows the following steps:

1. We explicit a continuous family  $(S_p)_{p \geq P(B)}$  of convex bodies which fill the upper boundary of the diagram.
2. We explicit a continuous family  $(L_p)_{p \geq P(B)}$  of convex bodies which fill the lower boundary of the diagram.
3. We use the latter domains to construct (via Minkowski sums) a family of continuous paths  $(\Gamma_p)_{p \geq P(B)}$  which relate upper domains to lower ones. By continuously increasing the perimeter, we show that we are able to cover all the area between the upper and lower boundaries.

#### Step 1: The upper boundary of the diagram:

The upper boundary corresponds to domains which are Cheeger of themselves, which means that  $C_\Omega = \Omega$ . It is shown in [20, Theorem 2] that stadiums (i.e. the convex hull of two identical disks) are Cheeger of themselves, we then use them to fill the upper boundary  $\{(x, x) \mid x \geq P(B)\}$ .

Let us consider the family of stadiums  $(Q_t)_{t \geq 0}$  given by convex hulls of the balls of unit radius centred in  $O(0, 0)$  and  $O_t(0, t)$  rescaled so as  $|Q_t| = 1$ . The function  $t \in [0, +\infty) \mapsto P(Q_t) = \frac{2(\pi+t)}{\sqrt{\pi+2t}}$  is continuous and strictly increasing. Thus, we have by the intermediate values Theorem:

$$\{(P(Q_t), h(Q_t)) \mid t \geq 0\} = \{(P(Q_t), P(Q_t)) \mid t \geq 0\} = \{(x, x) \mid x \geq P(B)\}.$$

#### Step 2: The lower boundary of the diagram:

Since equality (10) holds for sets that are homothetical to their form bodies, we use such domains to fill the lower boundary.

Let us consider the family  $(C_d)_{d \geq 2}$  of the so-called symmetrical cup-bodies, which are given by convex hulls of the unit ball (centred in  $O(0, 0)$  of radius 1) and the points of coordinates  $(-d/2, 0)$  and  $(d/2, 0)$  rescaled so as  $|C_d| = 1$ . By using formulae (7) and (8) of [17], we have for every  $d \geq 2$ :

$$P(C_d) = 2\sqrt{\sqrt{d^2 - 1} + 2 \arcsin \frac{2}{d}}.$$

The function  $d \in [2, +\infty) \mapsto P(C_d) = 2\sqrt{\sqrt{d^2 - 1} + 2 \arcsin \frac{2}{d}}$  is continuous and strictly increasing, this shows by the intermediate values Theorem that:

$$\{(P(C_d), h(C_d)) \mid d \geq 2\} = \{(P(C_t), P(C_t)/2 + \sqrt{\pi}) \mid d \geq 2\} = \{(x, x/2 + \sqrt{\pi}) \mid x \geq P(B)\}.$$

#### Step 3: Continuous paths:

Since the functions  $t \in [0, +\infty) \mapsto P(Q_t) = \frac{2(\pi+t)}{\sqrt{\pi+2t}}$  and  $d \in [2, +\infty) \mapsto P(C_d) = 2\sqrt{\sqrt{d^2 - 1} + 2 \arcsin \frac{2}{d}}$  are continuous and strictly increasing, we have that for every  $p \geq P(B)$  there exists a unique  $(t_p, d_p) \in [0, +\infty) \times [2, +\infty)$  such that  $P(Q_{t_p}) = P(C_{d_p}) = p$ : from now on we denote  $S_p := Q_{t_p}$  and  $L_p := C_{d_p}$ .

For every  $p \geq P(B)$ , we introduce the closed and continuous path  $\Gamma_p$ :

$$\begin{aligned} \Gamma_p &: [0, 3] \longrightarrow \mathbb{R}^2 \\ t &\longmapsto \begin{cases} (P(K_p^t), h(K_p^t)) & \text{if } t \in [0, 1], \\ ((t-1)P(B) + (2-t)p, (t-1)P(B) + (2-t)(p/2 + \sqrt{\pi})) & \text{if } t \in [1, 2], \\ ((t-2)P(B) + (3-t)p, (t-2)P(B) + (3-t)p) & \text{if } t \in [2, 3], \end{cases} \end{aligned}$$

where

$$K_p^t := \frac{tS_p + (1-t)L_p}{\sqrt{|tS_p + (1-t)L_p|}} \in \mathcal{K}_1^2.$$

The application  $t \in [0, 1] \mapsto tS_p + (1-t)L_p \in (\mathcal{K}^2, d^H)$  is continuous and since the measure is continuous for the Hausdorff distance, we deduce that  $t \in [0, 1] \mapsto K_p^t \in (\mathcal{K}_1^2, d^H)$  is continuous, thus by continuity of the

perimeter and the Cheeger constant for the Hausdorff distance, the path  $t \in [0, 3] \mapsto \Gamma_p(t) \in \mathbb{R}^2$  is a continuous curve.

Since the diameters of  $L_p$  and  $S_p$  are colinear, we can use the results of steps 1. and 3. of the proof of [?, Theorem 3.13], thus we have

$$\forall t \in [0, 1], \quad \frac{p}{2} \leq P(K_p^t) \leq p. \quad (11)$$

#### **Step 4: Stability of the paths:**

Now, we prove a continuity result on the paths  $(\Gamma_p)_{p \geq P(B)}$ : let us take  $p_0 \geq P(B)$  and  $\varepsilon > 0$ , we show that:

$$\exists \alpha_\varepsilon > 0, \forall p \in (p_0 - \alpha_\varepsilon, p_0 + \alpha_\varepsilon) \cap [P(B), +\infty), \quad \sup_{t \in [0, 3]} \|\Gamma_p(t) - \Gamma_{p_0}(t)\| \leq \varepsilon. \quad (12)$$

Let us take  $p \in [P(B), p_0 + 1]$ , with straightforward computations we have that for every  $t \in [1, 3]$ :

$$\|\Gamma_p(t) - \Gamma_{p_0}(t)\| \leq 2|p - p_0| \xrightarrow{p \rightarrow p_0} 0.$$

The remaining case ( $t \in [0, 1]$ ) requires more computations. For every  $t \in [0, 1]$ , we have

$$\|\Gamma_p(t) - \Gamma_{p_0}(t)\| \leq |P(K_p^t) - P(K_{p_0}^t)| + |h(K_p^t) - h(K_{p_0}^t)| \leq \underbrace{\left(2\pi + \frac{(p_0 + 1)^6}{2}\right)}_{C_{p_0 > 0}} d^H(K_p^t, K_{p_0}^t).$$

Indeed, we used:

- for the term with perimeters

$$|P(K_p^t) - P(K_{p_0}^t)| = \left| \int_0^{2\pi} h_{K_p^t} - \int_0^{2\pi} h_{K_{p_0}^t} \right| \leq 2\pi \times \|h_{K_p^t} - h_{K_{p_0}^t}\|_\infty = 2\pi \times d^H(K_p^t, K_{p_0}^t),$$

- the first assertion of Lemma 2.7 for the term with the Cheeger constants, with the sets  $K_p^t$  and  $K_{p_0}^t$  that we assume to contain the origin  $O$  and whose radial functions are denoted  $f_{p,t}, f_{p_0,t}$ .

$$\begin{aligned} |h(K_p^t) - h(K_{p_0}^t)| &\leq \frac{2}{\min(r(K_p^t), r(K_{p_0}^t))^2} \times \|f_{p,t} - f_{p_0,t}\|_\infty \quad (\text{by Lemma 2.7}) \\ &\leq \frac{2}{\min(r(K_p^t), r(K_{p_0}^t))^2} \times \frac{\|f_{p,t}\|_\infty \|f_{p_0,t}\|_\infty}{\min(r(K_p^t), r(K_{p_0}^t))^2} \times d^H(K_p^t, K_{p_0}^t) \quad (\text{by [5, Proposition 2]}) \\ &\leq \frac{(p_0 + 1)^6}{2} d^H(K_p^t, K_{p_0}^t) \quad (\text{we used } r(\Omega) \geq \frac{|\Omega|}{P(\Omega)} \text{ (see [7] for example) and } \|f\|_\infty \leq d(\Omega) \leq \frac{P(\Omega)}{2}). \end{aligned}$$

Moreover, we have:

$$\begin{aligned}
d^H(K_p^t, K_{p_0}^t) &= \|h_{K_p^t} - h_{K_{p_0}^t}\|_\infty \\
&= \left\| \frac{(1-t)h_{L_{p_0}} + th_{S_{p_0}}}{\sqrt{|(1-t)L_{p_0} + tS_{p_0}|}} - \frac{(1-t)h_{L_p} + th_{S_p}}{\sqrt{|(1-t)L_p + tS_p|}} \right\|_\infty \\
&\leq (1-t) \left\| \frac{h_{L_{p_0}}}{\sqrt{|(1-t)L_{p_0} + tS_{p_0}|}} - \frac{h_{L_p}}{\sqrt{|(1-t)L_p + tS_p|}} \right\|_\infty \\
&\quad + t \left\| \frac{h_{S_{p_0}}}{\sqrt{|(1-t)L_{p_0} + tS_{p_0}|}} - \frac{h_{S_p}}{\sqrt{|(1-t)L_p + tS_p|}} \right\|_\infty \\
&\leq \frac{1}{\sqrt{|(1-t)L_p + tS_p|}} \left( \|h_{S_{p_0}} - h_{S_p}\|_\infty + \|h_{L_{p_0}} - h_{L_p}\|_\infty \right) \\
&\quad + \left( \|h_{S_{p_0}}\|_\infty + \|h_{L_{p_0}}\|_\infty \right) \left| \frac{1}{\sqrt{|(1-t)L_p + tS_p|}} - \frac{1}{\sqrt{|(1-t)L_{p_0} + tS_{p_0}|}} \right| \\
&\leq (d^H(S_{p_0}, S_p) + d^H(L_{p_0}, L_p)) \\
&\quad + \left( \|h_{S_{p_0}}\|_\infty + \|h_{L_{p_0}}\|_\infty \right) \times \left| |(1-t)L_p + tS_p| - |(1-t)L_{p_0} + tS_{p_0}| \right| \\
&\leq (d^H(S_{p_0}, S_p) + d^H(L_{p_0}, L_p)) \\
&\quad + \underbrace{\left( \|h_{S_{p_0}}\|_\infty + \|h_{L_{p_0}}\|_\infty \right) \times \sum_{k=0}^2 |W_k(L_p, S_p) - W_k(L_{p_0}, S_{p_0})|}_{G(p, p_0) \xrightarrow{p \rightarrow p_0} 0}
\end{aligned}$$

Finally, we deduce that  $\lim_{p \rightarrow p_0} \sup_{t \in [0,3]} \|\Gamma_p(t) - \Gamma_{p_0}(t)\| = 0$ , which proves (12).

### Step 5: Conclusion:

Now that we proved that the boundaries  $\{(x, x) \mid x \geq P(B)\}$  and  $\{(x, x/2 + \sqrt{\pi}) \mid x \geq P(B)\}$  are included in the diagram  $\mathcal{D}_{\mathcal{K}^2}$ , it remains to show that it is also the case for the set of points contained between them. We argue by contradiction, assuming that there exists  $A(x_A, y_A) \in \{(x, y) \mid x > x_0 \text{ and } x/2 + \sqrt{\pi} < y < x\}$ , such that  $A \notin \mathcal{D}_{\mathcal{K}^2}$ .

We consider the function  $\phi_A : p \in [P(B), +\infty) \mapsto \text{ind}(\Gamma_p, A)$ , where  $\text{ind}(\Gamma_p, A)$  is the index of  $A$  with respect to  $\Gamma_p$  (also called the winding number of the closed curve  $\Gamma_p$  around the point  $A$ ).

- By Step 3 and continuity of the index, the function  $\phi_A$  is constant on  $[P(B), +\infty)$ .
- By the first inequality of (11), for every  $p \leq x_A$  the point  $A$  is in the exterior of  $\Gamma_p$ , thus  $\phi_A(p) = 0$ .
- On the other hand, By the second inequality of (11), for every  $p \geq 2x_A$ , the point  $A$  is in the exterior of  $\Gamma_p$ , thus  $\phi_A(p) \neq 0$ .

By the last three points we get a contradiction, thus  $A \in \mathcal{D}_{\mathcal{K}^2}$ . Finally, we get the equality

$$\mathcal{D}_{\mathcal{K}^2} = \left\{ (x, y) \mid x \geq x_0 \text{ and } \frac{1}{2}x + \sqrt{\pi} \leq y \leq x \right\}.$$

### 3.3 Proof of the first assertion of Theorem 1.1 (simply connected sets)

By inequalities (3) and (4) we have

$$\mathcal{D}_{\mathcal{S}^2} \subset \{(x_0, x_0)\} \cup \{(x, y) \mid x \geq x_0 \text{ and } 0 < y \leq x\}.$$

We have  $(x_0, x_0) = (P(B), h(B)) \in \mathcal{S}^2$ . Take  $(p, \ell) \in \{(x, y) \mid x > x_0 \text{ and } 0 < y \leq x\}$ , let us prove that there exists a simply connected domain  $\Omega \subset \mathbb{R}^2$  of unit area such that  $P(\Omega) = p$  and  $h(\Omega) = \ell$ .

If  $\ell \geq p/2 + \sqrt{\pi}$ , then by the second assertion of Theorem 1.1 there exists a convex (thus simply connected) domain satisfying the latter properties. Now, let us assume  $\ell < p/2 + \sqrt{\pi}$ : we take  $L_p$  as in the proof of the second assertion of Theorem 1.1 to be the convex hull of a disk and a point outside it such that  $h(L_p) = \ell$  and  $|L_p| = 1$ . As shown

in Figure 5, it is possible to continuously deform  $L_p$  in such a way to increase its perimeter while keeping constant its area and its Cheeger constant, thus there exists a simply connected set  $L'_p$  such that  $|L'_p| = 1$ ,  $P(L'_p) = p$  and  $h(L'_p) = \ell$ , which means that  $(p, \ell) \in \mathcal{D}_S$ .

Finally, we obtain the equality

$$\mathcal{D}_{S^2} = \{(x, y) \mid x \geq x_0 \text{ and } 0 < y \leq x\}.$$

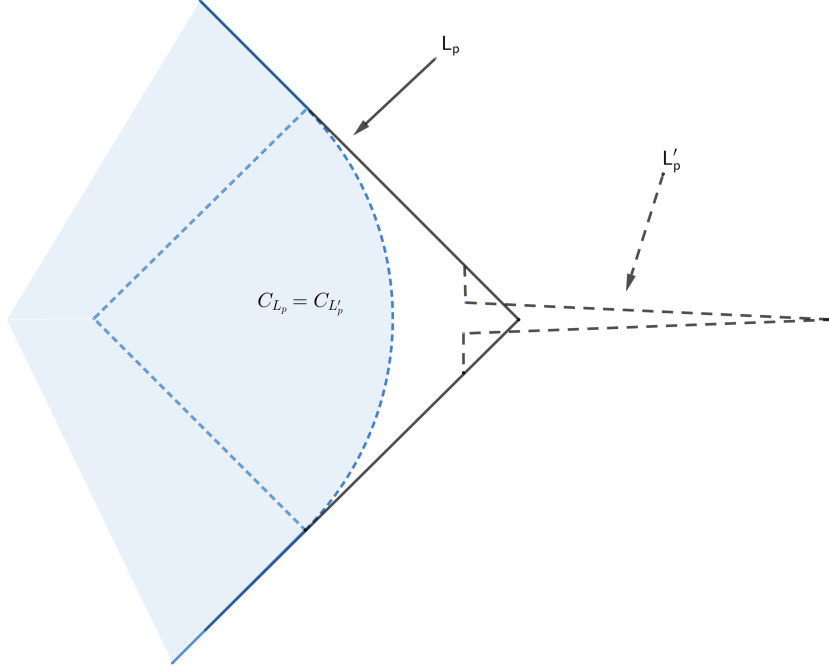


Figure 5: Tailed domain  $L'_p$  with the same area and Cheeger set and higher perimeter.

### 3.4 Proof of inequality (7)

This is a quite direct application of Lemma 2.5 and the inequality  $T(\Omega) \geq N \tan \frac{\pi}{N}$  (see Theorem 2.1). Indeed, for any  $\Omega \in \mathcal{P}_N$ , one has:

$$h(\Omega) \leq F(\Omega) = \frac{P(\Omega) + \sqrt{P(\Omega)^2 - 4(T(\Omega) - \pi)|\Omega|}}{2|\Omega|} \leq \frac{P(\Omega) + \sqrt{P(\Omega)^2 + 4(\pi - N \tan \frac{\pi}{N})|\Omega|}}{2|\Omega|}.$$

The first inequality is an equality if and only if  $\Omega$  is Cheeger-regular and the second one is an equality if and only if  $T(\Omega) = N \tan \frac{\pi}{N}$ , which is equivalent to  $\alpha_1 = \dots = \alpha_N = \frac{N-2}{2N}\pi$ .

### 3.5 Proof of Theorem 1.2

#### 3.5.1 If $N = 3$

We have by (6):

$$\forall \Omega \in \mathcal{P}_3, \quad \sqrt{|\Omega|}h(\Omega) = \frac{P(\Omega)}{2\sqrt{|\Omega|}} + \sqrt{\pi},$$

thus we have the inclusion:

$$\mathcal{D}_3 \subset \left\{ \left( x, \frac{x}{2} + \sqrt{\pi} \right) \mid x \geq P(R_3) \right\}.$$

The reverse inclusion is shown by considering for example the family  $(T_d)_{d \geq 1}$  of isosceles triangles of vertices  $X_d \left(0, \frac{\sqrt{3}}{2}\right)$ ,  $Y_d \left(\frac{d}{2}, 0\right)$  and  $Z_d \left(-\frac{d}{2}, 0\right)$ .

We have for every  $d \geq 1$ :

$$\begin{cases} P(R_3) = x_1 \leq x_d := \frac{P(T_d)}{\sqrt{|T_d|}} = \frac{d+\sqrt{d^2+3}}{\frac{3^{1/4}}{2}\sqrt{d}} \xrightarrow{d \rightarrow +\infty} +\infty \\ h(R_3) = y_1 \leq y_d := \frac{P(T_d)}{2\sqrt{|T_d|}} + \sqrt{\pi} = \frac{d+\sqrt{d^2+3}}{3^{1/4}\sqrt{d}} + \sqrt{\pi} \xrightarrow{d \rightarrow +\infty} +\infty, \end{cases}$$

where inequalities  $x_1 \leq x_d$  and  $y_1 \leq y_d$  are consequences of the isoperimetric inequality for triangles.

This shows by using the intermediate value Theorem, that:

$$\left\{ \left( \frac{P(T_d)}{|T_d|^{1/2}}, |T_d|^{1/2} h(T_d) \right) \mid d \geq 1 \right\} = \{(x_d, y_d) \mid d \geq 1\} = \left\{ \left( x, \frac{x}{2} + \sqrt{\pi} \right) \mid x \geq P(R_3) \right\} \subset \mathcal{D}_3,$$

thus, we obtain the equality

$$\mathcal{D}_3 = \left\{ \left( x, \frac{x}{2} + \sqrt{\pi} \right) \mid x \geq P(R_3) \right\}.$$

### 3.5.2 If $N$ is even

We have by inequalities (5) and (7):

$$\mathcal{D}_N \subset \left\{ (x, y) \mid x \geq P(R_N) \text{ and } \frac{x}{2} + \sqrt{\pi} \leq y \leq f_N(x) \right\},$$

where  $f_N : x \in [P(R_N), +\infty) \mapsto \frac{x + \sqrt{x^2 + 4(\pi - N \tan \frac{\pi}{N})}}{2}$ .

It remains to prove the reverse inclusion: we are able to provide explicit families of elements of  $\mathcal{P}_N$  that respectively fill the upper and lower boundaries of  $\mathcal{D}_N$  and then use those domains to construct continuous paths that fill the diagram.

#### Step 1: The upper boundary:

We recall that inequality (7) is an equality if and only if  $\Omega$  is Cheeger-regular and all its angles are equal to  $(N-2)\pi/N$ . A natural family of  $N$ -gons that satisfy those two properties is the one obtained by elongating two parallel sides of  $R_N$  (the regular  $N$ -gon of unit area). Note that the existence of two parallel sides is due to the fact that  $N$  is even. We parameterize this family via the diameters of its elements and denote it  $(U_\delta)_{\delta \geq d(R_N)}$ .

Since the map  $\delta \in [P(R_N), +\infty) \mapsto U_\delta \in (\mathcal{P}_N, d^H)$  is continuous, the perimeter and area are continuous for the Hausdorff distance  $d^H$ ,  $P(U_{d(R_N)}) = P(R_N)$  and

$$\frac{P(U_\delta)}{|U_\delta|^{1/2}} \geq \frac{P(U_\delta)}{\delta^{1/2} \times d(R_N)^{1/2}} \geq \frac{2\delta}{\delta^{1/2} \times d(R_N)^{1/2}} = \frac{2}{d(R_N)^{1/2}} \times \delta^{1/2} \xrightarrow{\delta \rightarrow +\infty} +\infty, \quad (13)$$

we deduce by the intermediate values Theorem that

$$\forall p \geq P(R_N), \exists \delta_p \geq d(R_N), \quad \frac{P(U_{\delta_p})}{|U_{\delta_p}|^{1/2}} = p.$$

Moreover, the sets  $(U_\delta)$  are Cheeger-regular and have all angles equal to  $(N-2)\pi/N$ , thus they all realise equality in (7) :

$$|U_\delta|^{1/2} h(U_\delta) = \frac{P(U_\delta) + \sqrt{P(U_\delta)^2 + 4(\pi - N \tan \frac{\pi}{N})|U_\delta|}}{2|U_\delta|^{1/2}} = f_N \left( \frac{P(U_\delta)}{\sqrt{|U_\delta|}} \right).$$

Finally, we deduce that the upper boundary of  $\mathcal{D}_N$  is given by the set of points  $\{(x, f_N(x)) \mid x \geq P(R_N)\}$ .

#### Step 2: The lower boundary:

As for the upper boundary's case we construct a continuous family of  $N$ -gons  $(V_\delta)_{\delta \geq d(R_N)}$ , such that  $V_{d(R_N)} = R_N$  and  $d(V_\delta) = \delta$  for every  $\delta \geq d(R_N)$ . We assume that the diameter of  $R_N$  is given by  $[OA]$ , where  $O = (0, 0)$  and  $A = (d(R_N), 0)$  and denote  $B_N$  its incircle (see Figure 6) and  $M_1, \dots, M_N$  its vertices.

Take  $\delta \geq d(R_N)$ , we denote  $A_\delta = (\delta, 0)$  and  $(\Delta_\delta), (\Delta'_\delta)$  the lines passing through  $A_\delta$  which are tangent to  $B_N$ . The line  $(\Delta_\delta)$  (resp.  $(\Delta'_\delta)$ ) cuts the boundary of  $R_N$  in two points: we denote  $M_{k_\delta}^\delta$  (resp.  $M_{N-k_\delta+1}^\delta$ ) the farthest one from  $A_\delta$  (see Figure 6), where  $k_\delta \in \llbracket 1, N/2 \rrbracket$  such that  $2k_\delta - 2$  is the number of vertices of  $R_N$  that are in the region given by the convex cone delimited by  $(\Delta_\delta)$  and  $(\Delta'_\delta)$ . We then define  $V_\delta$  as the (convex) polygon whose vertices are given by:



The diagram shows a central point  $O$  (marked with a blue 'x') and a red circle  $B_8$ . A blue polygon is inscribed within the circle. A green dashed line  $V_\delta$  is shown, representing a Voronoi edge. The diagram is divided into regions by dashed lines. Labels include  $O = M_1^\delta$ ,  $M_2^\delta$ ,  $M_3^\delta = M_4^\delta$ ,  $M_5^\delta = A_\delta$ ,  $M_6^\delta = M_7^\delta$ ,  $M_8^\delta$ ,  $(\Delta_\delta)$ ,  $(\Delta'_\delta)$ , and  $B_8$ .

Note that  $V_\delta$  has at most  $N$  sides and that it is a circumscribed polygon which means that it lays on the lower boundary of the diagram  $\mathcal{D}_N$ . We also, note that the applications  $\delta \in [P(R_N), +\infty) \mapsto M_k^\delta \in \mathbb{R}^2$  are continuous and thus it is also the case for  $\delta \in [P(R_N), +\infty) \mapsto V_\delta \in (\mathcal{P}_N, d^H)$ . Then, by similar estimates than (13) we get that  $\lim_{\delta \rightarrow +\infty} \frac{P(V_\delta)}{|V_\delta|^{1/2}} = +\infty$ , thus the lower boundary of  $\mathcal{D}_N$  is given by the set of points  $\{(x, x/2 + \sqrt{\pi}) \mid x \geq P(R_N)\}$ .

Now that we have two families  $(U_\delta)$  and  $(V_\delta)$  of extremal shapes, it remains to define continuous paths that relates the upper domains to the lower ones and fill the whole diagram. Unfortunately, unlike for the case of the class  $\mathcal{K}^2$ , one cannot use Minkowski sums as they increase the number of sides and thus could give polygons that are not in the class  $\mathcal{P}_N$ , we will then construct the paths by continuously mapping the lower and upper polygons vertices.

$$\forall t \in [0, 1], \quad \frac{P(\Omega_t^\delta)}{|\Omega_t^\delta|^{1/2}} \geq \frac{2\delta}{\delta^{1/2} \times d(R_N)^{1/2}} = \frac{2}{d(R_N)^{1/2}} \times \delta^{1/2}. \quad (14)$$

For every  $\delta \geq d(R_N)$ , we introduce the closed and continuous path  $\gamma_\delta$  :

$$\gamma_\delta : [0, 3] \longrightarrow \mathbb{R}^2$$

$$t \longmapsto \begin{cases} \left( \frac{P(\Omega_t^\delta)}{|\Omega_t^\delta|^{1/2}}, |\Omega_t^\delta|^{1/2} h(\Omega_t^\delta) \right) & \text{if } t \in [0, 1], \\ \left( (t-1)P(R_N) + (2-t)\frac{P(V_\delta)}{|V_\delta|^{1/2}}, (t-1)P(R_N) + (2-t)\frac{P(V_\delta)}{2|V_\delta|^{1/2}} + \sqrt{\pi} \right) & \text{if } t \in [1, 2], \\ \left( (t-2)P(R_N) + (3-t)\frac{P(U_\delta)}{|U_\delta|^{1/2}}, (t-2)P(R_N) + (3-t)\frac{P(U_\delta)}{|U_\delta|^{1/2}} \right) & \text{if } t \in [2, 3], \end{cases}$$

#### **Step 4: Stability of the paths:**

Take  $\delta_0 \geq d(R_N)$  and  $\varepsilon > 0$ , let us show that

$$\exists \alpha_\varepsilon > 0, \forall \delta \in (\delta_0 - \alpha_\varepsilon, \delta_0 + \alpha_\varepsilon) \cap [P(R_N), +\infty), \quad \sup_{t \in [0, 3]} \|\gamma_\delta(t) - \gamma_{\delta_0}(t)\| \leq \varepsilon. \quad (15)$$

Let us take  $\delta \in [d(R_N), \delta_0 + 1]$ , with straightforward computations we have that for every  $t \in [1, 3]$ :

$$\|\gamma_\delta(t) - \gamma_{\delta_0}(t)\| \leq 2 \min \left( \left| \frac{P(U_\delta)}{|U_\delta|^{1/2}} - \frac{P(U_{\delta_0})}{|U_{\delta_0}|^{1/2}} \right|, \left| \frac{P(V_\delta)}{|V_\delta|^{1/2}} - \frac{P(V_{\delta_0})}{|V_{\delta_0}|^{1/2}} \right| \right) \xrightarrow{\delta \rightarrow \delta_0} 0.$$

Moreover, by the quantitative estimates of Section 2, there exist constants  $C(\delta_0), C'(\delta_0) > 0$  depending only on  $\delta_0$  such that for all  $\delta \in [d(R_N), \delta_0 + 1]$  and all  $t \in [0, 1]$

$$\begin{aligned} \|\gamma_\delta(t) - \gamma_{\delta_0}(t)\| &\leq \left| \frac{P(\Omega_t^\delta)}{|\Omega_t^\delta|^{1/2}} - \frac{P(\Omega_t^{\delta_0})}{|\Omega_t^{\delta_0}|^{1/2}} \right| + \left| |\Omega_t^\delta|^{1/2} h(\Omega_t^\delta) - |\Omega_t^{\delta_0}|^{1/2} h(\Omega_t^{\delta_0}) \right| \\ &\leq C(\delta_0) \times \left( |P(\Omega_t^\delta) - P(\Omega_t^{\delta_0})| + \left| |\Omega_t^\delta| - |\Omega_t^{\delta_0}| \right| + |h(\Omega_t^\delta) - h(\Omega_t^{\delta_0})| \right) \\ &\leq C'(\delta_0) \times \max_{i \in \llbracket 1, N \rrbracket} \|(1-t)M_i^\delta + tL_i^\delta - (1-t)M_i^{\delta_0} - tL_i^{\delta_0}\| \\ &\leq C'(\delta_0) \times \max_{i \in \llbracket 1, N \rrbracket} (\|M_i^\delta - M_i^{\delta_0}\| + \|L_i^\delta - L_i^{\delta_0}\|) \xrightarrow{\delta \rightarrow \delta_0} 0. \end{aligned}$$

Finally, we deduce that  $\lim_{\delta \rightarrow \delta_0} \sup_{t \in [0, 3]} \|\gamma_\delta(t) - \gamma_{\delta_0}(t)\| = 0$ , which proves (15).

#### **Step 5: Conclusion:**

As for the case of convex sets, once we proved that the boundaries  $\{(x, f_N(x)) \mid x \geq P(R_N)\}$  and  $\{(x, x/2 + \sqrt{\pi}) \mid x \geq P(R_N)\}$  are included in the diagram  $\mathcal{D}_N$ , it remains to show that it is also the case for the zone between them. We argue by contradiction, assuming that there exists  $A(x_A, y_A) \in \{(x, y) \mid x > P(R_N) \text{ and } x/2 + \sqrt{\pi} < y < x\}$ , such that  $A \notin \mathcal{D}_N$ .

We consider the function  $\psi_A : \delta \in [d(R_N), +\infty) \mapsto \text{ind}(\gamma_\delta, A)$ , where  $\text{ind}(\gamma_p, A)$  is the index of  $A$  with respect to  $\gamma_\delta$  (also called the winding number of the closed curve  $\gamma_\delta$  around the point  $A$ ).

- By Step 4 and the continuity of the index, the function  $\psi_A$  is constant on  $[P(R_N), +\infty)$ .
- By the estimates above (step 4), for  $\delta$  sufficiently close to  $\delta_0$  the point  $A$  is in the interior of  $\gamma_\delta$ , thus  $\psi_A(\delta) = 0$ .
- On the other hand, by inequality (14), the point  $A$  is in the interior of  $\gamma_\delta$  for sufficiently high values of  $\delta$ , thus  $\psi_A(\delta) \neq 0$ .

By the last three points we get a contradiction, thus  $A \in \mathcal{D}_N$ . Finally, we get the equality

$$\mathcal{D}_N = \left\{ (x, y) \mid x \geq P(R_N) \text{ and } \frac{1}{2}x + \sqrt{\pi} \leq y \leq f_N(x) \right\}.$$

### **3.5.3 If $N$ is odd**

By inequalities (5) and (7), we have:

$$\mathcal{D}_N \subset \{(x, y) \mid x \geq P(R_N) \text{ and } x/2 + \sqrt{\pi} \leq y \leq f_N(x)\}.$$

Let us study the upper and lower boundaries of the diagram  $\mathcal{D}_N$ .

**Lower boundary:**

Since  $N - 1$  is even, we have by Section 3.5.2 that:

$$\{(x, x/2 + \sqrt{\pi}) \mid x \geq P(R_{N-1})\} \subset \mathcal{P}_{N-1} \subset \mathcal{P}_N.$$

It remains to prove that

$$\{(x, x/2 + \sqrt{\pi}) \mid x \in [P(R(N)), P(R_{N-1})]\} \subset \mathcal{P}_N.$$

To do so, we continuously move two consecutive sides of the polygon  $R_N$  so as to align them while keeping the polygon circumscribed, this gives us a continuous (for the Hausdorff distance) family  $(W_t)_{t \in [0,1]}$  of convex inscribed polygons such that  $W_0 = R_N$  and  $W_1$  is an element of  $\mathcal{P}_{N-1}$ , see Figure 7.

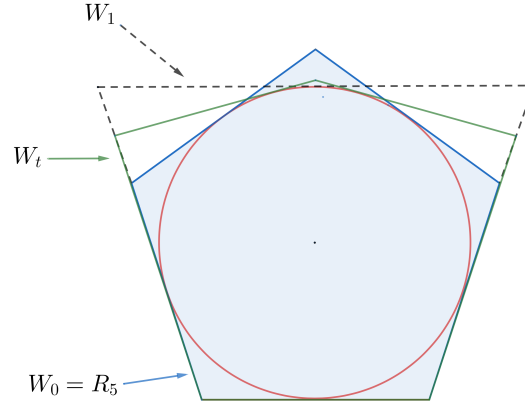


Figure 7: Construction of the circumscribed polygons  $W_t$ .

Since the map  $t \in [0, 1] \mapsto W_t \in (\mathcal{K}^2, d^H)$  is continuous, the functionals perimeter, area and Cheeger constant are continuous on  $(\mathcal{K}^2, d^H)$  and  $\frac{P(W_1)}{\sqrt{|W_1|}} \geq P(R_{N-1})$  (because of the polygonal isoperimetric inequality in  $\mathcal{P}_{N-1}$ ), we have by the intermediate values Theorem:

$$\{(x, x/2 + \sqrt{\pi}) \mid x \in [P(R_N), P(R_{N-1})]\} \subset \left\{ \left( \frac{P(W_t)}{\sqrt{|W_t|}}, \sqrt{|W_t|}h(W_t) \right) \mid t \in [0, 1] \right\} \subset \mathcal{D}_N.$$

We finally have:

$$\{(x, x/2 + \sqrt{\pi}) \mid x \in [P(R(N)), +\infty)\} \subset \mathcal{P}_N.$$

**Upper boundary:**

Let us now study the upper boundary. We introduce the function

$$\begin{aligned} g_N : [P(R_N), +\infty) &\longrightarrow \mathbb{R} \\ p &\longmapsto \sup \{h(\Omega) \mid \Omega \in \mathcal{P}_N, |\Omega| = 1 \text{ and } P(\Omega) = p\} \end{aligned} \quad (16)$$

First, let us prove that the problem  $\sup \{h(\Omega) \mid \Omega \in \mathcal{P}_N, |\Omega| = 1 \text{ and } P(\Omega) = p\}$  admits a solution, that we denote  $\Omega_p \in \mathcal{P}_N$ .

Take  $(\Omega_p^n)_{n \in \mathbb{N}}$  sequence of elements of  $\mathcal{P}_N$  such that  $|\Omega_p^n| = 1$  and  $P(\Omega_p^n) = p$  for every  $n \in \mathbb{N}$  which satisfies

$$\lim_{n \rightarrow +\infty} h(\Omega_p^n) = \sup \{h(\Omega) \mid \Omega \in \mathcal{P}_N, |\Omega| = 1 \text{ and } P(\Omega) = p\}.$$

Since the diameters of the sets  $(\Omega_p^n)$  are all bounded by  $p$  and the involved functionals are invariant by translations, we may assume without loss of generality that there exist a fixed ball  $D \subset \mathbb{R}^2$  that contains all the polygons  $\Omega_p^n$ . Let us denote  $A_1^n, \dots, A_N^n$  the vertices of  $\Omega_p^n$ , the sequences  $(A_1^n), \dots, (A_N^n)$  are bounded in  $\mathbb{R}^2$ , thus, by Bolzano-Weirstrass Theorem, there exist  $\sigma : \mathbb{N} \rightarrow \mathbb{N}$  strictly increasing and  $A_1, \dots, A_N \in \mathbb{R}^2$  such that  $\lim_{n \rightarrow +\infty} A_k^{\sigma(n)} = A_k$ . By elementary arguments of convex geometry one shows that the points  $A_1, \dots, A_N$  are the vertices of a convex polygon

$\Omega_p$  which is also the limit of  $(\Omega_p^{\sigma(n)})_n$  for Hausdorff distance. By the continuity of the perimeter, the volume and the Cheeger constant for the Hausdorff distance among convex sets, we have:

$$\begin{cases} |\Omega_p| = \lim_{n \rightarrow +\infty} |\Omega_p^{\sigma(n)}| = 1 \\ P(\Omega_p) = \lim_{n \rightarrow +\infty} P(\Omega_p^{\sigma(n)}) = p \\ h(\Omega_p) = \lim_{n \rightarrow +\infty} h(\Omega_p^{\sigma(n)}) = \sup \{h(\Omega) \mid \Omega \in \mathcal{P}_N, |\Omega| = 1 \text{ and } P(\Omega) = p\}. \end{cases}$$

Finally, we conclude that  $\Omega_p \in \mathcal{P}_N$  is a solution of the problem  $\sup \{h(\Omega) \mid \Omega \in \mathcal{P}_N, |\Omega| = 1 \text{ and } P(\Omega) = p\}$ .

Next, let us prove the stated properties of the function  $g_N$ .

### 1) The function $g_N$ is continuous

Let  $p_0 \in [P(R_N), +\infty)$

- We first show an superior limit inequality. Let  $(p_n)_{n \geq 1}$  real sequence converging to  $p_0$  such that

$$\limsup_{p \rightarrow p_0} h(\Omega_p) = \lim_{n \rightarrow +\infty} h(\Omega_{p_n}).$$

As the perimeter of  $(\Omega_{p_n})_{n \in \mathbb{N}^*}$  is uniformly bounded, one may assume that the domains  $(\Omega_{p_n})_{n \in \mathbb{N}^*}$  are included in a fixed ball: then by similar arguments than above,  $(\Omega_{p_n})$  converges to a convex polygon  $\Omega^* \in \mathcal{P}_N$  for the Hausdorff distance, up to a subsequence that we also denote  $p_n$  for simplicity.

Again, by the continuity of the perimeter, the volume and the Cheeger constant for the Hausdorff distance among convex sets, we have:

$$\begin{cases} |\Omega^*| = \lim_{n \rightarrow +\infty} |\Omega_{p_n}| = 1 \\ P(\Omega^*) = \lim_{n \rightarrow +\infty} P(\Omega_{p_n}) = \lim_{n \rightarrow +\infty} p_n = p_0 \\ h(\Omega^*) = \lim_{n \rightarrow +\infty} h(\Omega_{p_n}) = \limsup_{p \rightarrow p_0} h(\Omega_p) \end{cases}$$

Then by definition of  $g_N$  (since  $\Omega^* \in \mathcal{P}_N, |\Omega^*| = 1$  and  $P(\Omega^*) = p_0$ ), we obtain:

$$g_N(p_0) \geq h(\Omega^*) = \lim_{n \rightarrow +\infty} h(\Omega_{p_n}) = \limsup_{p \rightarrow p_0} h(\Omega_p) = \limsup_{p \rightarrow p_0} g_N(p).$$

- It remains to prove an inferior limit inequality. Let  $(p_n)_{n \geq 1}$  be a real sequence converging to  $p_0$  such that:

$$\liminf_{p \rightarrow p_0} g_N(p) = \lim_{n \rightarrow +\infty} g_N(p_n).$$

By using parallel chord movements (see the proof of Lemma 2.6), we can construct a sequence of unit area polygons  $(K_n)_{n \geq 1}$  with at most  $N$  sides, converging to  $\Omega_{p_0}$  for Hausdorff distance such that  $P(K_n) = p_n$  for sufficiently high values of  $n \in \mathbb{N}^*$ .

By using the definition of  $g_N$  one can write

$$\forall n \in \mathbb{N}^*, \quad g_N(p_n) \geq h(K_n).$$

Passing to the limit, we get:

$$\liminf_{p \rightarrow p_0} g_N(p) = \lim_{n \rightarrow +\infty} g_N(p_n) \geq \lim_{n \rightarrow +\infty} h(K_n) = h(\Omega_{p_0}) = g_N(p_0).$$

As a consequence we finally get  $\lim_{p \rightarrow p_0} g_N(p) = g_N(p_0)$ , so  $g_N$  is continuous on  $[P(R_N), +\infty)$ .

### 2) The function $g_N$ is strictly increasing

Let us assume by contradiction that  $g_N$  is not strictly increasing, then there exist  $p_2 > p_1 \geq P(R_N)$  such that  $g_N(p_2) < g_N(p_1)$ , and from the equality case in the polygonal isoperimetric inequality, we necessarily have  $p_1 > P(R_N)$ . Since  $g$  is continuous, it reaches its maximum on  $[P(R_N), p_2]$  at a point  $p^* \in (P(R_N), p_2)$ , that is to say

$$\forall \Omega \in \mathcal{P}_N \text{ such that } |\Omega| = 1 \text{ and } P(\Omega) \in [P(R_N), p_2], \quad h(\Omega_{p^*}) = g_N(p^*) \geq h(\Omega). \quad (17)$$

We note that  $g_N(p^*) > p^*/2 + \sqrt{\pi}$ , indeed if it is not the case (i.e  $g_N(p^*) = p^*/2 + \sqrt{\pi}$ ) we have for  $h > 0$  :

$$g_N(p^* + h) \geq (p^* + h)/2 + \sqrt{\pi} > p^*/2 + \sqrt{\pi} = g_N(p^*),$$

this contradicts the fact that  $g_N$  admits a local maximum at  $p^*$ .

(17) shows that  $\Omega_{p^*}$  is a local maximizer of the Cheeger constant between convex  $N$ -gons of unit area. On the other hand, the fact that  $h(\Omega_{p^*}) = g_N(p^*) > \frac{P(\Omega_{p^*}) + \sqrt{4\pi|\Omega_{p^*}|}}{2|\Omega_{p^*}|}$  implies that  $\Omega_{p^*}$  is not a circumscribed polygon. Let us now show that any non-circumscribed polygon  $\Omega$  (ie.  $T(\Omega) < \frac{P(\Omega)^2}{4|\Omega|}$ ) could be perturbed (while preserving the number of sides) in such a way to increase  $|\Omega|^{1/2}h(\Omega)$ .

We denote  $(\ell_i)_{i \in \llbracket 1; N \rrbracket}$  the lengths of the sides of the polygon  $\Omega$  and  $(\alpha_i)_{i \in \llbracket 1; N \rrbracket}$  its inner angles and denote

$$r_0 := \min_{1 \leq i \leq N} \frac{\ell_i}{\tan\left(\frac{\pi}{2} - \frac{\alpha_i}{2}\right) + \tan\left(\frac{\pi}{2} - \frac{\alpha_{i-1}}{2}\right)}$$

We distinguish two cases:

- If  $|\Omega| - r_0 P(\Omega) + r_0^2 (T(\Omega) - \pi) \geq 0$ , this means by [20, Theorem 3] that there exists a side of  $\Omega$  that does not touch the Cheeger set  $C_\Omega$  or touch it in one point. We consider a parallel displacement of this side as shown in Figure 8. For  $\varepsilon > 0$  sufficiently small, the polygons  $\Omega$  and  $\Omega_\varepsilon$  have the same Cheeger set, thus we have  $|\Omega_\varepsilon|^{1/2}h(\Omega_\varepsilon) > |\Omega|^{1/2}h(\Omega)$ .

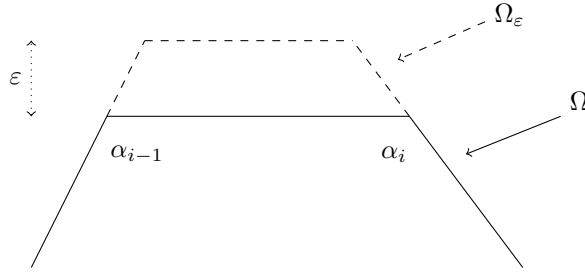


Figure 8: Parallel displacement of one side.

- On the other hand if  $|\Omega| - r_0 P(\Omega) + r_0^2 (T(\Omega) - \pi) < 0$ , then by [20, Theorem 3], the polygons  $\Omega$  and  $\Omega_\varepsilon$  (for  $|\varepsilon|$  sufficiently small) are Cheeger-regular and thus we have an explicit expression of their Cheeger constants.

We have for  $|\varepsilon|$  sufficiently small

$$|\Omega_\varepsilon|^{1/2}h(\Omega_\varepsilon) = \frac{P(\Omega_\varepsilon) + \sqrt{P(\Omega_\varepsilon)^2 - 4(T(\Omega_\varepsilon) - \pi)|\Omega_\varepsilon|}}{\sqrt{|\Omega_\varepsilon|}} = \frac{P(\Omega_\varepsilon)}{\sqrt{|\Omega_\varepsilon|}} + \sqrt{\frac{P(\Omega_\varepsilon)^2}{|\Omega_\varepsilon|} - 4(T(\Omega) - \pi)}, \quad (18)$$

where we used  $T(\Omega) = T(\Omega_\varepsilon)$  for the last equality.

As stated in the proof of [9, Lemma 23] through elementary geometric arguments, we have

$$\begin{cases} P(\Omega_\varepsilon) &= P(\Omega) + \left( \frac{1}{\tan \alpha_{i-1}} + \frac{1}{\tan \alpha_i} + \frac{1}{\sin \alpha_{i-1}} + \frac{1}{\sin \alpha_i} \right) \times \varepsilon, \\ |\Omega_\varepsilon| &= |\Omega| + \ell_i \times \varepsilon + \frac{1}{2} \left( \frac{1}{\tan \alpha_{i-1}} + \frac{1}{\tan \alpha_i} \right) \times \varepsilon^2. \end{cases}$$

Thus :

$$\begin{aligned} \frac{P(\Omega_\varepsilon)^2}{|\Omega_\varepsilon|} &= \frac{\left( P(\Omega) + \left( \frac{1}{\tan \alpha_{i-1}} + \frac{1}{\tan \alpha_i} + \frac{1}{\sin \alpha_{i-1}} + \frac{1}{\sin \alpha_i} \right) \times \varepsilon \right)^2}{|\Omega| + \ell_i \times \varepsilon + \frac{1}{2} \left( \frac{1}{\tan \alpha_{i-1}} + \frac{1}{\tan \alpha_i} \right) \times \varepsilon^2} \\ &= \frac{P(\Omega)^2}{|\Omega|} + P(\Omega) \underbrace{\left( 2 \left( \frac{1}{\tan \alpha_{i-1}} + \frac{1}{\tan \alpha_i} + \frac{1}{\sin \alpha_{i-1}} + \frac{1}{\sin \alpha_i} \right) - \frac{P(\Omega)}{|\Omega|} \ell_i \right)}_{\Psi_i} \times \varepsilon + o_{\varepsilon \rightarrow 0}(\varepsilon). \end{aligned}$$

Let us show that there exists  $i \in \llbracket 1; N \rrbracket$  such that  $\Psi_i \neq 0$ . We assume by contradiction that  $\Psi_i = 0$  for every  $i \in \llbracket 1; N \rrbracket$ , we then have

$$\sum_{i=1}^N \Psi_i = 0,$$

which is equivalent to

$$P(\Omega) = \frac{4|\Omega|}{P(\Omega)} \times \sum_{i=1}^N \left( \frac{1}{\tan \alpha_i} + \frac{1}{\sin \alpha_i} \right) = \frac{4|\Omega|}{P(\Omega)} \times \sum_{i=1}^N \frac{1}{\tan \frac{\alpha_i}{2}} = \frac{4|\Omega|}{P(\Omega)} \times T(\Omega).$$

As stated in Theorem 2.1, this equality holds if and only if  $\Omega$  is a circumscribed polygon, which is not the case as assumed above. Thus, there exists  $i \in \llbracket 1; N \rrbracket$  such that  $\Psi_i \neq 0$ , then by performing a parallel displacement (in the suitable sense) of the  $i^{\text{th}}$  side, one is able to strictly increase  $P(\Omega)/|\Omega|^{1/2}$  which by (18) increases  $|\Omega|^{1/2}h(\Omega)$ .

### 3) Comparison between $g_N$ and $f_N$ and asymptotic

- It is immediate by the inclusion  $\mathcal{P}_{N-1} \subset \mathcal{P}_N$  and inequality (7) that  $f_{N-1} \leq g_N \leq f_N$  on  $[P(R_N), +\infty)$ .
- If we perform parallel displacement of one of the sides of the regular polygon  $R_N$  we obtain a continuous (for Hausdorff distance) family of Cheeger regular polygons  $(\Omega_\varepsilon)_{\varepsilon \in [0, \varepsilon_0]}$  with the same angles as  $R_N$  such that  $P(\Omega_\varepsilon)|\Omega_\varepsilon|^{1/2} > P(\Omega)|\Omega|^{1/2}$  for every  $\varepsilon \in (0, \varepsilon_0)$ , this proves that there exists  $b_N \geq P(\Omega_{\varepsilon_0})/|\Omega_{\varepsilon_0}|^{1/2} > P(R_N)$  such that for every  $p \in [P(R_N), b_N]$  we have  $g_N(p) = \frac{p + \sqrt{p^2 + 4(\pi - N \tan \frac{\pi}{N})}}{2} = f_N(p)$ .
- Let us prove that if  $\Omega$  is a unit area polygon of  $N$  sides whose angles are all equal (to  $\beta_N := \frac{N-2}{2N}\pi$ ), one has

$$P(\Omega) \leq \frac{2N}{\sqrt{\tan \frac{\beta_N}{2}}} \quad (19)$$

Let us assume that  $\Omega \subset \{y \geq 0\}$  and its longest side is given by the segment  $[OA]$  where  $A(\ell, 0)$  and  $\ell > 0$ . Since  $N$  is odd and all the angles of  $\Omega$  are equal, we deduce that there exists a unique vertex  $B(x_B, \eta)$  which is strictly higher (ie. has the largest ordinate) than all other vertices. We can assume without loss of generality that  $x_B \geq \ell/2$ . As shown in Figure 9, by convexity of  $\Omega$ , the line obtained by extending the left side of extremity  $B$  intersects the axis of abscissa in a point  $C(x_C, 0)$  such that  $x_C \leq 0$ .

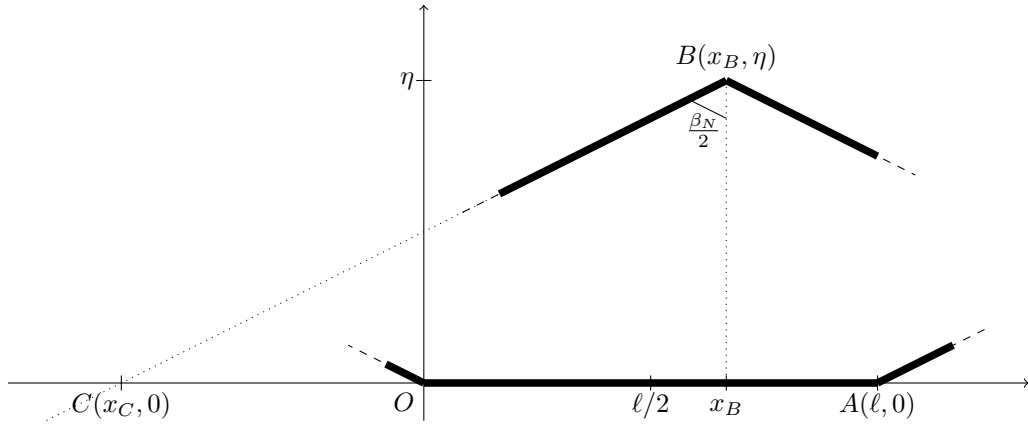


Figure 9: An  $N$ -gon with all angles equal to  $\beta_N$ .

We have

$$\frac{1}{\tan \frac{\beta_N}{2}} = \cotan \frac{\beta_N}{2} = \frac{\eta}{x_B - x_C} = 2 \frac{\frac{1}{2}\ell\eta}{\ell(x_B - x_C)} = 2 \frac{\mathcal{S}_{OAB}}{\ell(x_B - x_C)} \leq \frac{4}{\ell^2},$$

where the last inequality is a consequence of  $\mathcal{S}_{OAB} \leq 1$  (because  $OAB \subset \Omega$ ) and  $x_B - x_C \geq x_B \geq \ell/2$ .

Thus, we have the result

$$P(\Omega) \leq N\ell \leq \frac{2N}{\sqrt{\tan \frac{\beta_N}{2}}}.$$

This proves that there is no polygon of unit area,  $N$  sides and perimeter larger than  $\frac{2N}{\sqrt{\tan \frac{\beta_N}{2}}}$  whose inner angles are all equal (to  $\beta_N$ ).

Thus for every  $\Omega \in \mathcal{P}_N$  such that  $|\Omega| = 1$  and  $P(\Omega) \geq \frac{2N}{\sqrt{\tan \frac{\beta_N}{2}}}$ , we have

$$h(\Omega) \leq \frac{P(\Omega) + \sqrt{P(\Omega)^2 - 4(T(\Omega) - \pi)|\Omega|}}{2|\Omega|} < \frac{P(\Omega) + \sqrt{P(\Omega)^2 + 4(\pi - N \tan \frac{\pi}{N})|\Omega|}}{2|\Omega|} = f_N(P(\Omega)),$$

where the first inequality is (7) and the second (strict) one is a consequence of Theorem 2.1.

We finally have that:

$$\forall p > \frac{2N}{\sqrt{\tan \frac{\beta_N}{2}}}, \quad g_N(p) < f_N(p).$$

- Since  $N \geq 4$ , we have

$$\forall x \geq P(R_{N-1}), \quad \frac{x + \sqrt{x^2 + 4(\pi - (N-1) \tan \frac{\pi}{N-1})}}{2} = f_{N-1}(x) \leq g_N(x) \leq f_N(x).$$

Thus

$$g_N(x) \underset{x \rightarrow +\infty}{\sim} x.$$

## 4 Numerical simulations

Since it does not seem to be easy to explicitly find the upper boundary of the diagram  $\mathcal{D}_N$  when  $N$  is odd, we perform some simulations in order to have an approximation of the function  $g_N$ ; we numerically solve the following problems:

$$\max \{h(\Omega) \mid \Omega \in \mathcal{P}_N, \quad |\Omega| = 1 \text{ and } P(\Omega) = p_0\}, \quad (20)$$

where  $p_0 \in [P(R_N), +\infty)$ .

### 4.1 Parameterization of the domains

we parameterize a polygon  $\Omega$  via its vertices' coordinates  $A_1(x_1, y_1), \dots, A_N(x_N, y_N)$ .

- Let us first express the constraint of convexity in terms of the coordinates of the vertices of  $\Omega$ . It is classical that  $\Omega$  is convex if and only if all the interior angles are less than or equal to  $\pi$ . By using the cross product (see [2] for example), this, is equivalent to the constraints

$$C_k(x_1, \dots, x_N, y_1, \dots, y_N) := (x_{k-1} - x_k)(y_{k+1} - y_k) - (y_{k-1} - y_k)(x_{k+1} - x_k) \leq 0,$$

for  $k = 1, \dots, N$ , where we used the conventions  $A_0 = A_N$  and  $A_{N+1} = A_1$ .

- The volume and the perimeter of  $\Omega$  are given by the following formulae

$$\begin{cases} f(x_1, \dots, x_N, y_1, \dots, y_N) := P(\Omega) = \sum_{k=1}^N \sqrt{(x_{k+1} - x_k)^2 + (y_{k+1} - y_k)^2}, \\ g(x_1, \dots, x_N, y_1, \dots, y_N) := |\Omega| = \frac{1}{2} \left| \sum_{k=1}^N (x_k y_{k+1} - x_{k+1} y_k) \right| \end{cases}$$

- Finally, we introduce the function

$$\phi : (x_1, \dots, x_N, y_1, \dots, y_N) \mapsto \begin{cases} h(\Omega) & \text{if the polygon } \Omega \text{ does not have overlapping sides} \\ -1 & \text{if the polygon } \Omega \text{ does have overlapping sides} \end{cases}$$

where  $\Omega$  is the polygon of vertices  $A_1(x_1, y_1), \dots, A_N(x_N, y_N)$ . The Cheeger constant is computed by using an open source code of Benjamin Bogosel [4] based on the results of [20].

We are now able to write the Problem (20) in the following form

$$\begin{cases} \sup_{(x_1, \dots, y_N) \in \mathbb{R}^{2N}} \phi(x_1, \dots, y_N), \\ \forall k \in \llbracket 1, N \rrbracket, \quad C_k(x_1, \dots, x_N, y_1, \dots, y_N) \leq 0, \\ f(x_1, \dots, x_N, y_1, \dots, y_N) = p_0 \\ g(x_1, \dots, x_N, y_1, \dots, y_N) = 1. \end{cases}$$

## 4.2 Computation of the gradients

We want to use Matlab's routine `fmincon` to solve the last problem, to do so we should compute the gradients of the constraints  $C_k, f, g$  and the objective function  $\phi$ .

$C_k, f, g$  are explicitly expressed via usual functions of  $(x_1, \dots, y_N)$ , we then have by easy computations explicit formulae for the gradients. This is not the case for the objective function  $\phi$ . We use the following shape derivative formula of the Cheeger constant proved in [25]:

$$h'(\Omega, V) := \lim_{t \rightarrow 0} \frac{h(\Omega_t) - h(\Omega)}{t} = \frac{1}{|C_\Omega|} \int_{\partial C_\Omega \cap \partial \Omega} (-h(\Omega)) \langle V, n \rangle d\mathcal{H}^1,$$

where  $V \in \mathbb{R}^2 \rightarrow \mathbb{R}^2$  is a smooth perturbation,  $\Omega_t = (Id + tV)(\Omega)$ ,  $n(x)$  is the normal to  $\partial\Omega$  at the point  $x$  and is the curvature of  $\partial\Omega$  at the point  $x$ .

Since  $\Omega$  is a convex polygon and  $C_\Omega$  is  $C^{1,1}$ , we have  $\mathcal{K}^2 \text{ appa} = 0$  on  $\partial C_\Omega \cap \partial \Omega$ . Thus, if we denote  $V_{x_k}$  and  $V_{y_k}$  the perturbations respectively associated to the variables  $x_k$  and  $y_k$ , where  $k \in \llbracket 1, N \rrbracket$ , we have :

$$\begin{cases} \frac{\partial \phi}{\partial x_k}(x_1, \dots, x_N, y_1, \dots, y_N) = -\frac{h(\Omega)}{|C_\Omega|} \int_{\partial C_\Omega \cap \partial \Omega} \langle V_{x_k}, n \rangle d\mathcal{H}^1, \\ \frac{\partial \phi}{\partial y_k}(x_1, \dots, x_N, y_1, \dots, y_N) = -\frac{h(\Omega)}{|C_\Omega|} \int_{\partial C_\Omega \cap \partial \Omega} \langle V_{y_k}, n \rangle d\mathcal{H}^1 \end{cases}$$

## 4.3 Results

In Figure 10, we plot the points corresponding to  $10^5$  random convex pentagons and the points corresponding to the optimal pentagons obtained for  $p_0 \in \{P(R_5) + 0.02 \times k \mid k \in \llbracket 1, 100 \rrbracket\}$ , in addition to the curves representing Inequalities (3) and (7). We note (as proved in Theorem 1.2) that for small values of  $p_0$ , the points corresponding to the optimal domains are exactly located on the curve of the function  $f_5$  (that represents inequality (7)) which is no longer the case for those corresponding to larger values of  $p_0$ .

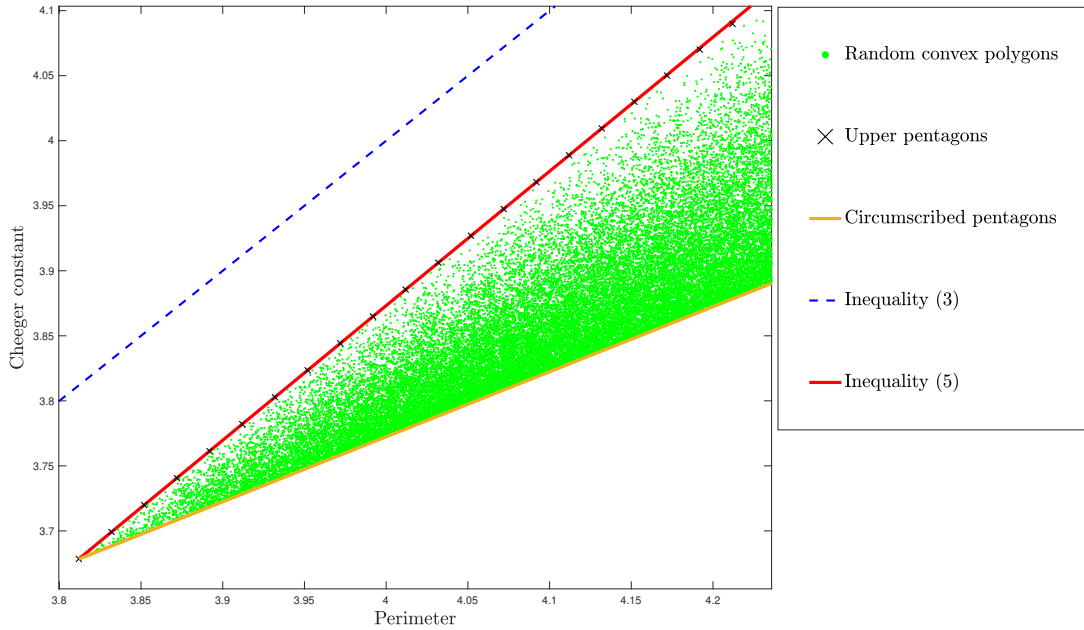


Figure 10: Blaschke-Santaló diagram of convex pentagons.



We give in the Figure 11 a zoom on the upper boundary, where one notes that the points corresponding to the upper pentagons are at first exactly located on the red curve corresponding to inequality (7) and then come off and become strictly lower than it. We numerically note that the abscissa  $b_5$  introduced in the statement of Theorem 1.2 is indeed (as proven in the present paper) bounded from above by  $\frac{10}{\sqrt{\tan \frac{3\pi}{20}}}$ .

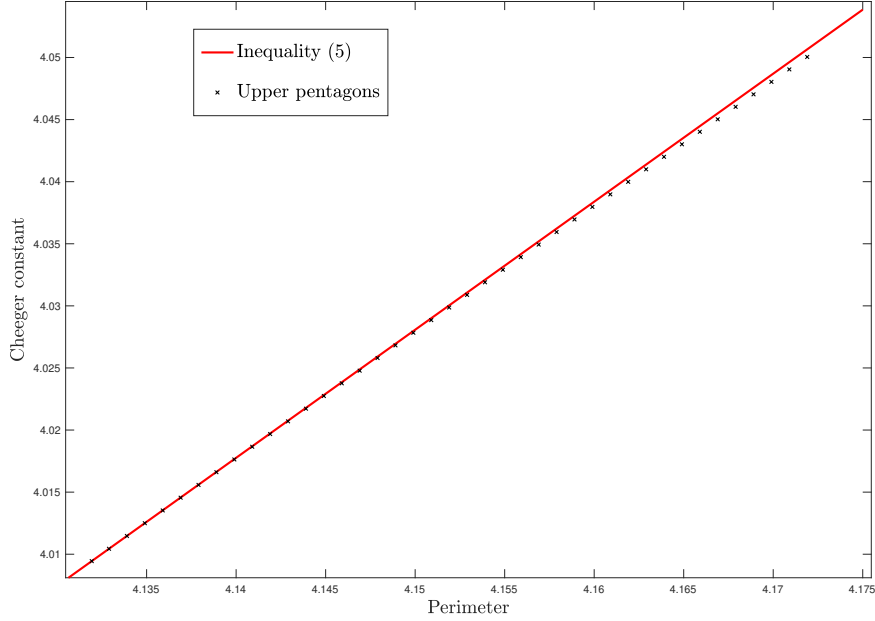


Figure 11: A zoom on the upper boundary.

Finally, we give the obtained optimal shapes for  $p_0 \in \{3.86, 4, 5\}$ . We note that for larger values of  $p_0$  the maximizers seem not to be Cheeger-regular.

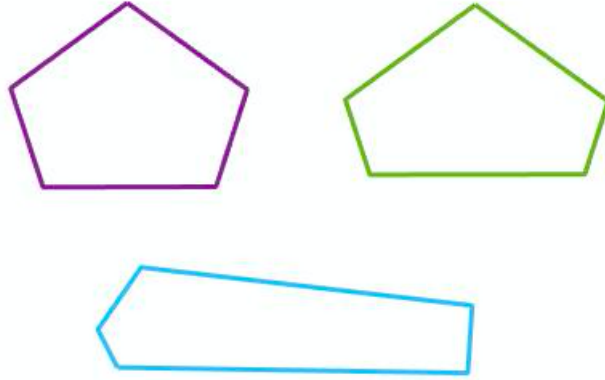


Figure 12: Optimal pentagons obtained for  $p_0 \in \{3.86, 4, 5\}$ .

**Remark 4.1.** Our numerical approach is validated by testing it on the cases for which we have a theoretical description of the boundary, namely:

- The lower boundary of the diagrams  $\mathcal{D}_N$ , where  $N \geq 3$ , which is given as stated in Theorem 1.2 by:

$$\{(x, x/2 + \sqrt{\pi}) \mid x \geq P(R_N)\}.$$

- The upper boundary of the diagrams  $\mathcal{D}_N$ , where  $N$  is even, which is given as stated in Theorem 1.2 by:

$$\left\{ \left( x, \frac{x + \sqrt{x^2 + 4(\pi - N \tan \frac{\pi}{N})}}{2} \right) \mid x \geq P(R_N) \right\}.$$

In both cases, satisfying results were obtained.

## 5 Some applications

We give some applications of the results and ideas developed in this paper.

### 5.1 First application

One early result in the spirit of inequality (5) is due to R. Brooks and P. Waksman, see Theorem 5.1 below. It gives a lower estimate of the Cheeger constant of convex polygons, which we show to be a consequence inequality (5).

**Proposition 5.1.** [8, Th 3.] *If  $\Omega$  is a convex polygon, we denote  $\Omega^*$  the (unique up to rigid motions) circumscribed polygon which has the same area as  $\Omega$  and whose angles are the same as those of  $\Omega$ , then*

$$h(\Omega) \geq h(\Omega^*) = \frac{\sqrt{T(\Omega)} + \sqrt{\pi}}{\sqrt{|\Omega|}}, \quad (21)$$

with equality if and only if  $\Omega = \Omega^*$  (up to rigid motions).

*Proof.* We show inequality (5) gives an alternative proof.

$$h(\Omega) \geq \frac{P(\Omega) + \sqrt{4\pi|\Omega|}}{2|\Omega|} \geq \frac{2\sqrt{|\Omega|}\sqrt{T(\Omega)} + \sqrt{4\pi|\Omega|}}{2|\Omega|} = \frac{\sqrt{T(\Omega)} + \sqrt{\pi}}{\sqrt{|\Omega|}} = \frac{\sqrt{T(\Omega^*)} + \sqrt{\pi}}{\sqrt{|\Omega^*|}},$$

where we respectively used (5) and (8) for the first and second inequalities and the fact that  $\Omega^*$  has the same area and angles as  $\Omega$  for the last equality. By Theorem 2.1 the second inequality is an equality if and only if  $\Omega$  is circumscribed, in this case the first inequality becomes also an equality.

On the other hand, since  $\Omega^*$  is an inscribed polygon, we have  $T(\Omega^*) = P(\Omega^*)^2/(4|\Omega^*|)$  (by Theorem 2.1) and  $h(\Omega^*) = \frac{P(\Omega^*) + \sqrt{4|\Omega^*|}}{2|\Omega^*|}$ .

Thus:

$$\frac{\sqrt{T(\Omega^*)} + \sqrt{\pi}}{\sqrt{|\Omega^*|}} = h(\Omega^*).$$

This ends the proof. □

### 5.2 Second application: on the stability of the Cheeger constant of polygons

We use inequality (5) and [10, Proposition 2.1] to give a quantitative version of the Faber-Krahn type inequality for convex polygons:

**Proposition 5.2.** *Take  $N \geq 3$ . There exists a positive constant  $C_N$  such that for every convex unit area  $N$ -gon  $\Omega$  there exists a rigid motion  $\rho$  of  $\mathbb{R}^2$  such that*

$$h(\Omega)^2 - h(\Omega_N)^2 \geq C_N d^H(\Omega, \rho(\Omega_N))^2. \quad (22)$$

*Proof.* Take  $N \geq 3$  and a  $N$ -gon  $\Omega$ , we have by inequality (5)

$$P(\Omega) \leq 2(h(\Omega) - \sqrt{\pi}) \quad \text{and} \quad P(\Omega_N) = 2(h(\Omega_N) - \sqrt{\pi}),$$

thus

$$\begin{aligned} P(\Omega)^2 - P(\Omega_N)^2 &\leq 4(h(\Omega) - \sqrt{\pi})^2 - 4(h(\Omega_N) - \sqrt{\pi})^2 \\ &= 4(h(\Omega)^2 - h(\Omega_N)^2 - 2\sqrt{\pi}(h(\Omega) - h(\Omega_N))) \\ &\leq 4(h(\Omega)^2 - h(\Omega_N)^2), \end{aligned}$$

where the last inequality is a consequence of the polygonal Faber-Krahn type inequality  $h(\Omega) \geq h(\Omega_N)$ .

On the other hand, it is proved in [10, Proposition 2.1], that there exists  $C_N > 0$  depending only on  $N$  such that

$$P(\Omega)^2 - P(\Omega_N)^2 \geq 4C_N d^H(\Omega, \rho(\Omega_N))^2,$$

combining with the latest inequality we get the announced result. □

**Remark 5.3.** *The quantitative inequality (22) shows in particular the stability of the Cheeger constant in the neighborhood of regular polygons between convex polygons with the same number of sides, in the sense that if the Cheeger constant of a convex polygon is close to the one of the unit area regular polygon with the same number of sides, then the polygon looks (up to rigid motions) like the latter one. A similar result can be obtained for non convex  $N$ -gons, see [11].*

## References

- [1] F. Alter and V. Caselles. Uniqueness of the Cheeger set of a convex body. *Nonlinear Anal.*, 70(1):32–44, 2009.
- [2] S. Bartels and G. Wachsmuth. Numerical approximation of optimal convex shapes. *SIAM J. Sci. Comput.*, 42(2):A1226–A1244, 2020.
- [3] W. Blaschke. Konvexe Bereiche gegebener konstanter Breite und kleinsten Inhalts. *Math. Ann.*, 76(4):504–513, 1915.
- [4] B. Bogosel. [https://github.com/bbogo/Cheeger\\_patch](https://github.com/bbogo/Cheeger_patch).
- [5] A. Boulkhémair. On a shape derivative formula in the Brunn-Minkowski theory. *SIAM J. Control Optim.*, 55(1):156–171, 2017.
- [6] L. Brasco. On principal frequencies and inradius in convex sets. *Bruno Pini Math. Anal. Semin.*, page 20, 2018.
- [7] L. Brasco. On principal frequencies and isoperimetric ratios in convex sets. *Ann. Fac. Sci. Toulouse Math.*, page 25, 2019.
- [8] R. Brooks and P. Waksman. The first eigenvalue of a scalene triangle. *Proc. Amer. Math. Soc.*, 100(1):175–182, 1987.
- [9] D. Bucur and I. Fragalà. A Faber-Krahn inequality for the Cheeger constant of  $N$ -gons. *J. Geom. Anal.*, 26(1):88–117, 2016.
- [10] M. Caroccia and F. Maggi. A sharp quantitative version of Hales’ isoperimetric honeycomb Theorem. *J. Math. Pures Appl. (9)*, 106(5):935–956, 2016.
- [11] M. Caroccia and R. Neumayer. A note on the stability of the Cheeger constant of  $N$ -gons. *J. Convex Anal.*, 22(4):1207–1213, 2015.
- [12] J. Cheeger. A lower bound for the smallest eigenvalue of the Laplacian. In *Problems in analysis (Papers dedicated to Salomon Bochner, 1969)*, pages 195–199. 1970.
- [13] S. J. Cox and M. Ross. Extremal eigenvalue problems for starlike planar domains. *J. Differential Equations*, 120(1):174–197, 1995.
- [14] G. Crasta, I. Fragalà, and F. Gazzola. A sharp upper bound for the torsional rigidity of rods by means of web functions. *Arch. Ration. Mech. Anal.*, 164(3):189–211, 2002.
- [15] A. Figalli, F. Maggi, and A. Pratelli. A note on Cheeger sets. *Proc. Amer. Math. Soc.*, 137(6):2057–2062, 2009.
- [16] A. Henrot and M. Pierre. *Shape variation and optimization*, volume 28 of *EMS Tracts in Mathematics*. European Mathematical Society (EMS), Zürich, 2018.
- [17] M. A. Hernández Cifre and G. Salinas. Some optimization problems for planar convex figures. Number 70, part I, pages 395–405. 2002. IV International Conference in “Stochastic Geometry, Convex Bodies, Empirical Measures & Applications to Engineering Science”, Vol. I (Tropea, 2001).
- [18] M.A. Hernandez Cifre, G. Salinas, and S.S Gomis. Complete systems of inequalities. *Journal of inequalities in pure and applied mathematics*, 2(1), March 2001.
- [19] V. Julin and G. Saracco. Quantitative lower bounds to the euclidean and the gaussian cheeger constants, 2020.
- [20] B. Kawohl and T. Lachand-Robert. Characterization of Cheeger sets for convex subsets of the plane. *Pacific J. Math.*, 225(1):103–118, 2006.
- [21] G. P. Leonardi, R. Neumayer, and G. Saracco. The Cheeger constant of a Jordan domain without necks. *Calc. Var. Partial Differential Equations*, 56(6):Paper No. 164, 29, 2017.

- [22] G. P. Leonardi and A. Pratelli. On the Cheeger sets in strips and non-convex domains. *Calc. Var. Partial Differential Equations*, 55(1):Art. 15, 28, 2016.
- [23] G. P. Leonardi and G. Saracco. Minimizers of the prescribed curvature functional in a Jordan domain with no necks. *ESAIM Control Optim. Calc. Var.*, 26:Paper No. 76, 20, 2020.
- [24] E. Parini. An introduction to the Cheeger problem. *Surv. Math. Appl.*, 6:9–21, 2011.
- [25] E. Parini and N. Saintier. Shape derivative of the cheeger constant. *ESAIM Control, Optimisation and Calculus of Variations*, 21, 2015.
- [26] L. Santaló. Sobre los sistemas completos de desigualdades entre treselementos de una figura convexa plana. *Math. Notae*, 17:82–104, 1961.
- [27] R. Schneider. *Convex Bodies: The Brunn-Minkowski Theory*. Cambridge University Press, 2nd expanded edition edition, 2013.